Ullmann Coupling Reactions on Gold Nanoparticles

(Expanding the Toolbox of Organic Synthesis)

Inauguraldissertation zur Erlangung des Doktorgrades (Dr. rer. nat.)
der Naturwissenschaftlichen Fachbereiche im Fachgebiet Chemie
der Justus-Liebig-Universität Gießen

vorgelegt von

Nathaniel Ukah

aus Nigeria

Betreuer: Prof. Dr. Hermann A. Wegner

Gießen 2024

Versicherung Nach §17 der Promotionsordnung

Ich erkläre: Ich habe die vorgelegte Dissertation selbstständig und ohne unerlaubte fremde Hilfe und nur mit den Hilfen angefertigt, die ich in der Dissertation angegeben habe. Alle Textstellen, die wörtlich oder sinngemäß aus veröffentlichten Schriften entnommen sind, und alle Angaben, die auf mündlichen Auskünften beruhen, sind als solche kenntlich gemacht. Ich stimme einer evtl. Überprüfung meiner Dissertation durch eine Antiplagiat-Software zu. Bei den von mir durchgeführten und in der Dissertation erwähnten Untersuchungen habe ich die Grundsätze guter wissenschaftlicher Praxis, wie sie in der „Satzung der Justus-Liebig-Universität Gießen zur Sicherung guter wissenschaftlicher Praxis“ niedergelegt sind, eingehalten.

Nathaniel Ukah Ort, Datum

Dekan:	Prof. Dr. Thomas Wilke
Erstgutachter:	Prof. Dr. Hermann A. Wegner
Zweitgutachter:	Prof. Dr. Bernd Smarsly

"Be kind and spread love everywhere you go. Let no one ever come to you without leaving happier."

Mother Teresa

Table of Contents

Abstract

Ullmann coupling has proven to be a useful tool for constructing C−C bonds. However, the most prominent disadvantage of Ullmann coupling is the poor selectivity between homo and hetero-Ullmann products. In 2021, the research groups of Wegner and Schirmeisen found a breakthrough towards solving this long-standing problem, using organic on-surface synthesis. However, be it as good as it may seem, this technique is limited to surfaces with flat geometries to enable visualization of single molecules using Atomic Force Microscope (AFM). This stringent requirement limited the availability of the coupled products to few molecules, which is far less than that obtained via traditional in-solution Ullmann coupling.

Therefore, in this work, and in analogy to the ultra-high vacuum on-surface synthesis, a new strategy for conducting organic reactions is developed. This strategy translates the 2D on-surface synthesis into 3D on-surface synthesis, adopts the high degree of selectivity obtained from 2D organic on-surface synthesis and enables the synthesis of large amounts of molecules (relative to the well-known 2D on-surface syntheses).

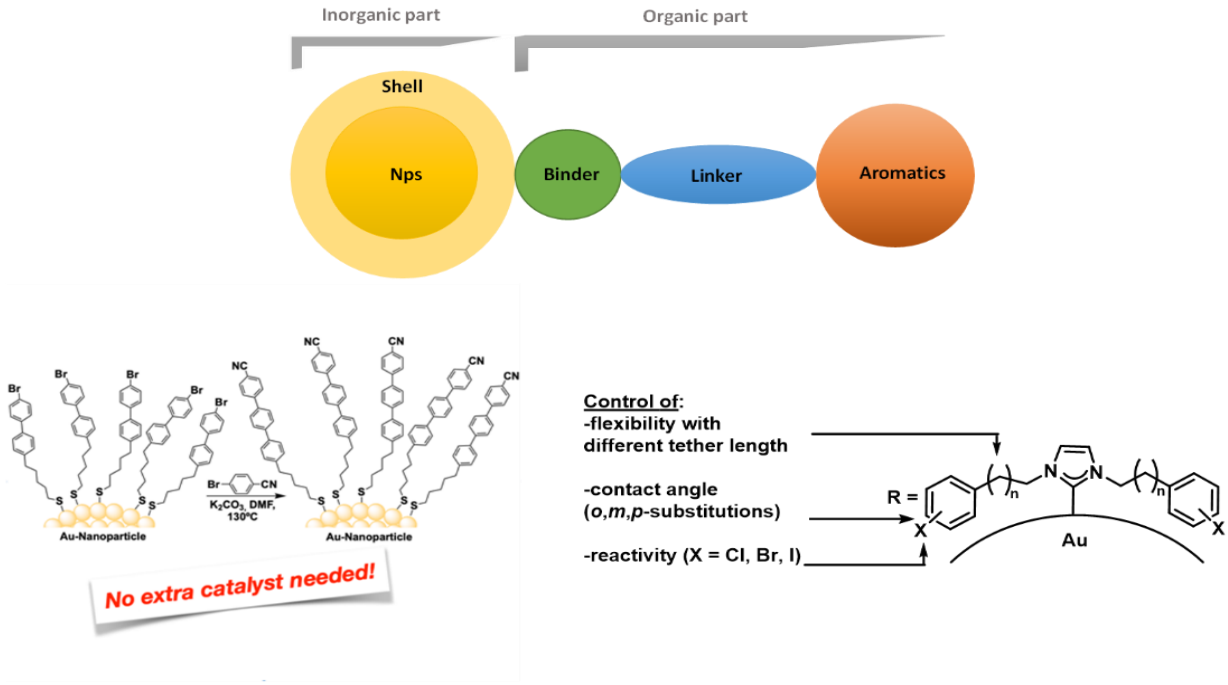

Figure 1. Selectivity towards hetero- and homo-Ullmann reaction using varied ligands.[1]

In addition, it also circumvents both disdavantages obtained from the previously outlined approaches in Ullmann reactions. This developed strategy involves attaching the coupling unit (in the form of a ligand) to a 3D gold surface, to form a hybrid material, bearing the catalyst and the reacting partner, all combined in one entity. The adopted geometry of these ligands on a 3D gold surface was exploited in swapping the natural selectivity of Ullmann reaction, thus, favoring hetero over homo Ullmann coupling reactions.

In a follow-up project, the different segments of the hybrid material were fine-tuned, and the binding group was changed from a π-donor ligand to a σ-donor ligand. This changed the entire bonding strength to the Au surface, bonding geometry and chemical reactivity of the reacting molecules attached to the Au surface. Thus, enabling a transferrence of on-surface synthesis from 2D to 3D surface, while giving rise to enhanced selectivity towards intermolecular homo Ullmann reaction.

Zusammenfassung

Die Ullmann-Kupplung hat sich als nützliches Werkzeug zur Herstellung von C-C-Bindungen erwiesen. Der größte Nachteil der Ullmann-Kupplung ist jedoch die schlechte Selektivität zwischen Homo- und Hetero-Ullmann-Produkten. Im Jahr 2021 gelang den Forschergruppen von Wegner und Schirmeisen mit der organischen On-Surface-Synthese ein Durchbruch zur Lösung dieses langjährigen Problems. Allerdings ist diese Technik, so gut sie auch sein mag, auf Oberflächen mit flacher Geometrie beschränkt, um die Visualisierung einzelner Moleküle mit dem Rasterkraftmikroskop (AFM) zu ermöglichen. Diese strenge Anforderung beschränkt die Verfügbarkeit der gekoppelten Produkte auf wenige Moleküle, was weit weniger ist als bei der traditionellen Ullmann-Kopplung in Lösung.

Daher wird in dieser Arbeit in Analogie zur Ultrahochvakuum-Oberflächensynthese eine neue Strategie zur Durchführung organischer Reaktionen entwickelt. Mit dieser Strategie wird die 2D-Oberflächensynthese in eine 3D-Oberflächensynthese umgewandelt, die hohe Selektivität der organischen 2D-Oberflächensynthese übernommen und die Synthese großer Mengen von Molekülen ermöglicht (im Vergleich zu den bekannten 2D-Oberflächensynthesen).

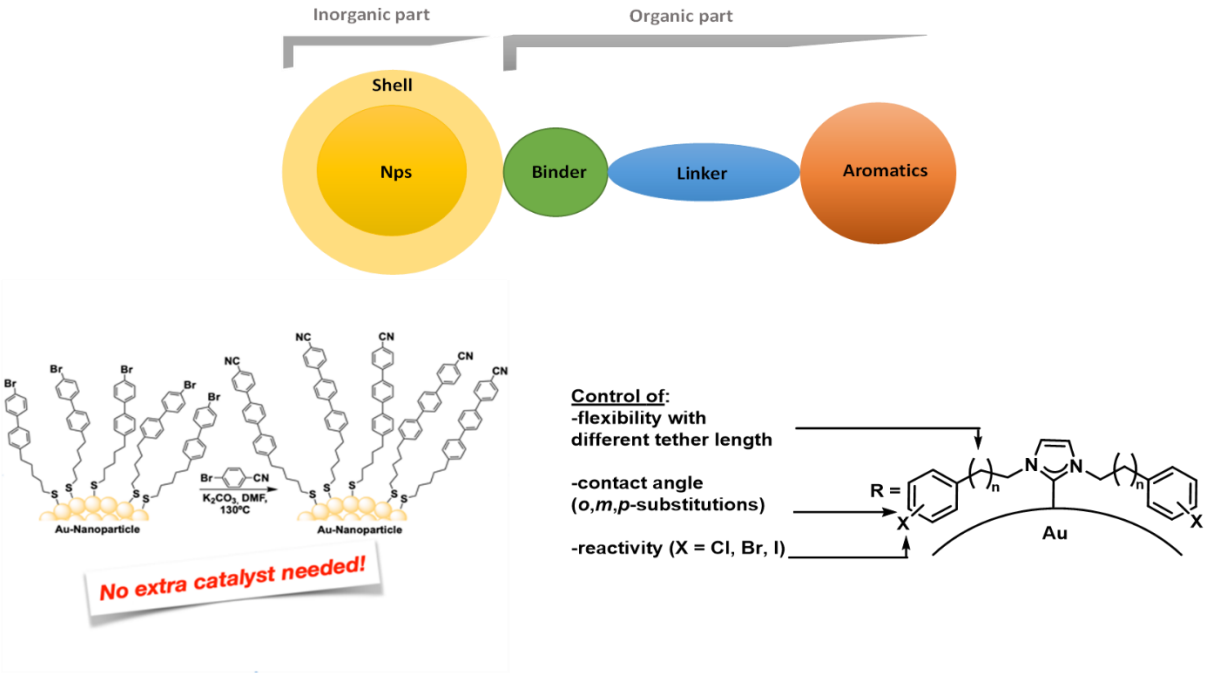

Abbildung 1. Selektivität bei der Hetero- und Homo-Ullmann-Reaktion unter Verwendung verschiedener Liganden.[1]

Darüber hinaus umgeht sie die beiden Nachteile, die sich aus den zuvor beschriebenen Ansätzen für Ullmann-Reaktionen ergeben. Bei dieser entwickelten Strategie wird die Kopplungseinheit (in Form eines Liganden) an eine 3D-Goldoberfläche angebracht, um ein Hybridmaterial zu bilden, das den Katalysator und den Reaktionspartner in einer Einheit vereint. Die angenommene Geometrie dieser Liganden auf einer 3D-Goldoberfläche wurde ausgenutzt, um die natürliche Selektivität der Ullmann-Reaktion zu verändern und so Hetero- gegenüber Homo-Ullmann-Kopplungsreaktionen zu begünstigen.

In einem Folgeprojekt wurden die verschiedenen Segmente des Hybridmaterials feinabgestimmt und die Bindungsgruppe von einem π-Donor-Liganden zu einem σ-Donor-Liganden geändert. Dadurch änderte sich die gesamte Bindungsstärke zur Au-Oberfläche, die Bindungsgeometrie und die chemische Reaktivität der reagierenden Moleküle an der Au-Oberfläche. Dies ermöglichte eine Verlagerung der On-Surface-Synthese von der 2D- auf die 3D-Oberfläche und führte gleichzeitig zu einer erhöhten Selektivität für die intermolekulare Homo-Ullmann-Reaktion.

1 Introduction to Gold Nanoparticles

Gold Nanoparticles (AuNps) first appeared in history as soluble gold around the 5th century B.C. in Egypt and China.[2] However, scientific research on colloidal gold began with Michael Faraday's report on the formation of deep red solutions of gold in water by the reduction of an aqueous solution of gold salts using phosphorus in CS_2.[3] Since then, many different methods for the preparation of AuNps have been reported, these range from various top-down approaches (such as wet and dry grinding)[4] to bottom-up approaches (such as sol-gel and impregnation methods).[5] Among all these different approaches developed for the fabrication of AuNps, wet chemistry has proven to be the preferred choice, because of its relative simplicity, possible scale-up and use of inexpensive tools towards the miniaturization of Au materials.[6] The goal of such syntheses involves fine-tuning some salient parameters such as size, shape and uniformity, which are ultimately the prevailing factors behind their physical, chemical, optical, electronic and catalytic properties. However, the prepared Nps, invariably carry a layer of organic or inorganic material – usually in the form of organic ligand or capping agent - that provides them with added properties that could enhance the colloidal stability, and reactivity of the entire Np. Additionally, this ligand of functionalization plays an essential role to determining the nanoparticles physical, chemical, optical, electronic and catalytic properties, which in turn designate their final applications.[7] It is in this context that the choice of a right capping agent or ligand becomes essential. Since the applications of AuNps in various fields have substantially increased during the past few decades, it is of primary importance to understand the prevailing influence of the ligand during synthesis and on the final properties of interest. One of the relevant properties of AuNps is based on the presence of intense absorption and scattering in the visible and Near Infrared (NIR) spectral regions, which is the origin of the observed brilliant colors of AuNps when dispersed in solution.[8] Such special optical response results from the collective oscillation of surface electrons, in resonance with the frequency of the incident or applied electromagnetic radiation, which is known as localized surface plasmon resonance (LSPR).[7,9] The LSPR frequency - and thus the color of the AuNps - mainly depend on particle size, shape, ligands of functionalization, the dielectric nature of the surrounding solvent molecules and inter-particle distance.[7,9] For example, as the sizes of AuNps decrease, the distance between the valence and conduction bands increases, more energy will be needed to promote the

electrons from the valence band to the conducting bands, resulting to a blueshift or complete disappearance of the LSPR band.[9] For this reason, AuNps with core diameters below 2 nm do not display LSPRs, while AuNps in water with average diameters of 9, 15, 22, 48, and 99 nm, display LSPR maxima that are centered at 517, 520, 521, 533, and 575 nm, respectively.[2]

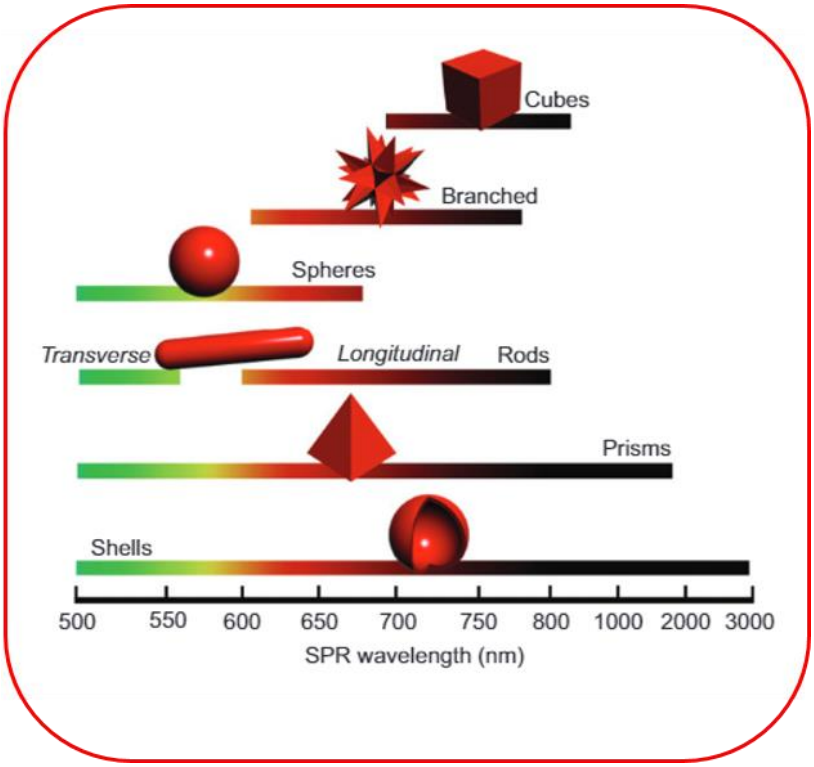

Figure 2. Correlation of SPR bands with shapes of AuNps. Reproduced with permission from ref.[10] Copyright © 2008, Springer Nature.

The shapes of AuNps even have a more pronounced effect on the optical properties than that of the sizes of the AuNps (Figure 2).[11,12] For example, the anisotropy of non-spherical AuNps leads to multiple possible LSPR modes.[7] Rod-like-shaped AuNps can accommodate two well differentiated resonance modes, due to oscillation of electrons across and along the long axis of the nanorod resulting to the so-called transverse and longitudinal modes respectively, the latter being extremely sensitive to the aspect ratio of the rod.[13] Interestingly, three main resonance modes have been identified when these Nps are changed from rod-like to triangular-shaped AuNps.[14] In these and other non-spherical Nps, a common feature is that the main plasmon resonance is red-shifted with respect to that of spherical nanoparticles, at 520 nm (Figure 2).[15] Hence, by tuning the morphology of AuNps, one can readily tune the LSPR frequency and multiplicity mode of the Nps in a wide spectral range, as

schematically depicted in Figure 2. However, in the context of this work, more emphasis will be placed on spherical AuNps as this geometry enables organic reactivity on surfaces. Nonetheless, another important parameter that could enhance the application of the AuNp is the inter-particle distance. When two or more Nps are in close proximity to each other, usually within 2.5 times the particle diameter,[16] their localized surface plasmon resonances could couple, leading to broadening and a red-shift of the single particle LSPR band.[12] Also, this coupling leads to the formation of so-called 'hot-spots' which are small gaps between adjacent particles exhibiting large electromagnetic field enhancements.[7] This coupling has been theoretically modeled,[17] and also applied towards Surface Enhanced Raman Scattering (SERS),[18] optoelectronics,[19] as well as in chemo and bio-sensors.[20]

Besides the ligand of functionalization, another parameter that could affect the applications of AuNps is the dielectric nature of the immediate surroundings, including the dispersing solvent medium.[21] Early work by Papavassiliou and coworkers has revealed a strong dependence of the position, intensity, and shape of absorption peaks on the dielectric constant of the medium surrounding the metal nanomaterials, by analyzing the optical properties of the Np films when immersed in solvents of different refractive indexes.[22] In this case, Au films appeared red when exposed to air but red-blue when immersed in CS_2, and linear relationships were found between the square of the maximum wavelength and the dielectric constant of the medium.[22]

However, it is the various ligands of functionalization or the capping agent used during the synthesis that actually plays the fundamental role in tuning the size, shape, morphology, the LSPR wavelength range, as well as the colloidal stability and functional versatility of the Nps, thus, determining their final applications.[7,11,13]

1.1 Syntheses of AuNps

AuNps can be synthesized either from the top-down approach or through bottom-up approach (Figure 3). The top-down method requires starting from bulk gold material and narrowing it down to the AuNp. This can be sub-divided into dry and wet grinding. In the dry grinding method, the solid substance is pulverized via application of a shock, or by compression using a jet mill or a hammer mill.[6] AuNps obtained via this technique are subject to aggregation due to increase in their surface energy.[6] Since

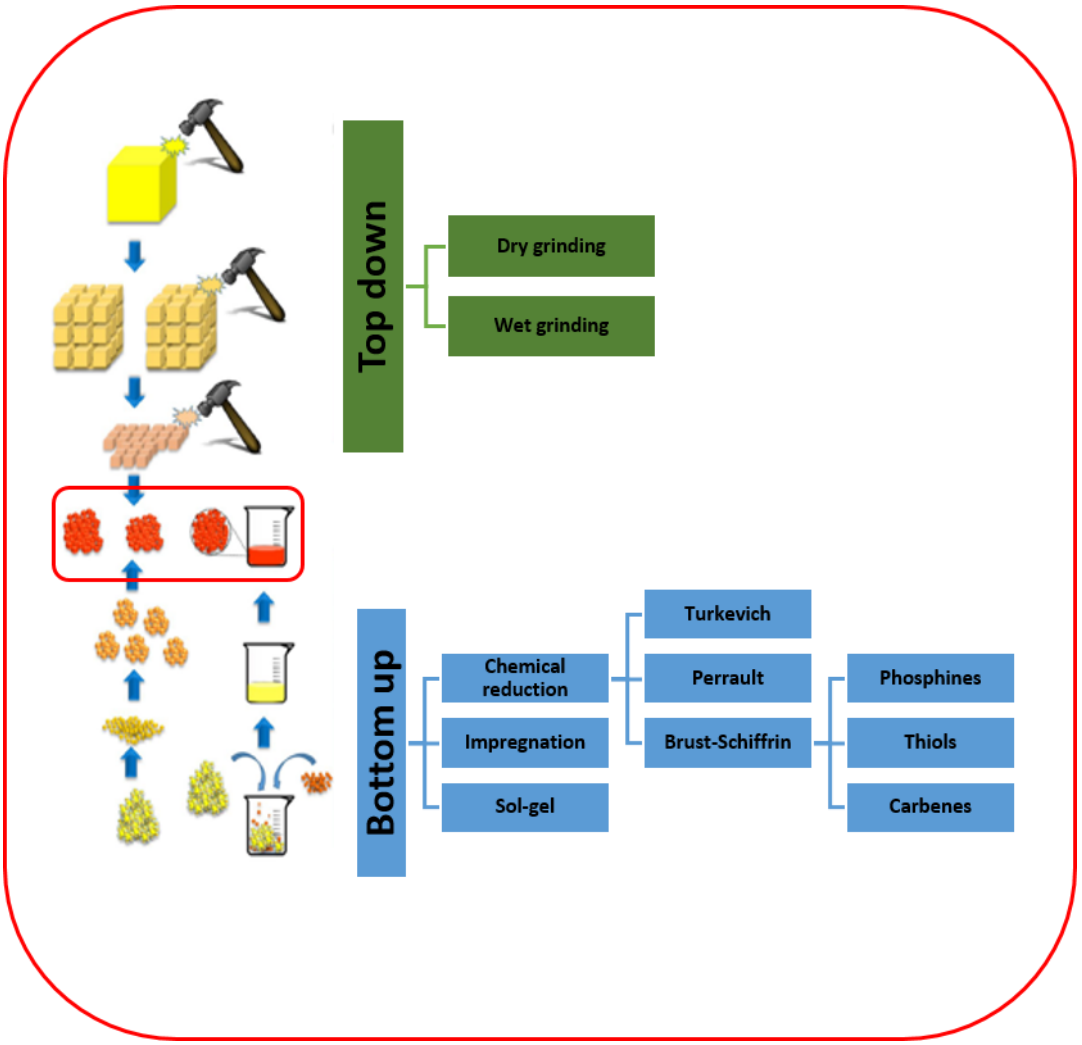

Figure 3. Different approaches towards the synthesis of AuNps Reproduced with permission from ref.[6] Copyright © 2015, Wiley-VCH Verlag GmbH & Co. KGaA.

condensation of small particles also takes place simultaneously with pulverization, it is difficult to obtain Np sizes of less than 300 nm by dry grinding.[6] On the other hand, wet grinding of a solid substrate is carried out using a tumbling ball mill, or a planetary ball mill.[6] Unlike the dry grinding method, the wet process is suitable for preventing the condensation of the Nps formed, and offers a possibility of obtaining relatively highly dispersed AuNps.[7,8] However, it is usually difficult to control the sizes of the formed AuNps using this technique, and these downsides have limited the use of the top-down approach.

Conversely, the bottom-up method involves the mixing of ions, complexes or molecules to undergo chemical transformations that convert them to the AuNps. This technique is dominated by liquid-phase methods which are further subdivided into sol-gel method, impregnation methods and the use of chemical reducing agents (Figure 3).

The sol-gel technique involves the hydrolysis of alkoxides or halide precursors at higher temperatures followed by calcination to furnish the metal oxide Nps.[23] This technique is preferred when control of homogeneity is a strong requirement for the Np.[23] On the other hand, impregnation method involves the mixing of the metal precursors (usually nitrates) at lower temperatures followed by calcination at high temperature to obtain the metal Np. The chemical reduction technique involves the use of varied reducing agents to obtain different sizes of AuNps. The principal advantage is the facile fabrication of Nps of various shapes, such as nanorods, nanowires, nanoprisms, nanoplates, and hollow Nps which is obtainable using different reducing agents.[8] With the chemical reduction method, it is possible to fine-tune the shape and size of the Nps by varying the reducing agent, the aging time, the dispersing agent, the overall reaction time and the reaction temperature.[8,13] This technique is further subdivided into the Turkevich method, Perrault method and the Brust-Schiffrin technique. Turkevich method adopts the usage of citrate salt as both the reducing agent and the capping agent.[24,25] The formation of uniform AuNps is revealed by a deep wine red color observed after ~10 minutes.[6] The average diameter of the Np can be tuned over quite a wide range (~10-100 nm) by varying the concentration ratio between the Au salt and the sodium citrate.[24] However, deviation from a spherical shape is normally observed for Nps larger than 30 nm, as well as a larger polydispersity of the obtained Np, thus, limiting the usage of this method.[24] In addition, the surface chemistry of the obtained AuNps is poorly defined, since citrate is easily degraded during synthesis and the binding of citrate to the Au surface is by mere adsorption.[6,13] The lack of availability of smaller sized Nps using the Turkevich method gave rise to a modification of this technique, known as the Perrault method. This technique uses hydroquinone to reduce $HAuCl_4$, giving rise to relatively smaller-sized Nps in the range of 15 nm.[26] Given the aforementioned importance of sizes of AuNps to its application, there was further need to narrow this size regime to a smaller scale and this gave rise to the Brust-Schiffrin method of AuNp syntheses which was developed by Schiffrin and coworkers (Scheme 1).[27] In this technique, $HAuCl_4$ is dissolved in water and subsequently transported into the organic phase using tetraoctylammonium bromide (TOAB) as the phase transfer agent. The thiolated ligand is then introduced into the mixture while reducing the stirring speed to 50 rpm until the solution turns colourless. This colourless Au^+ intermediate is finally reduced to Au^0 using an excess of sodium borohydride in a rapid stirring speed of 1200 rpm. The particle size obtained via this

technique can be tuned between 5 to 10 nm by varying the ratio of the thiolated ligand to the Au precursor, thus, offering added advantages in size control, over the other above-described techniques. Nonetheless, it is noteworthy to mention that this technique is not a panacea to all Np syntheses but limited to spherically-shaped thiol-functionalized AuNps. Having explained the use of thiols as ligands for stabilizing AuNps, it is of utmost importance to understand the nature of the Au-thiol bonding which facilitates its usage as a stabilizing ligand. This will be explained in the follow-up chapter.

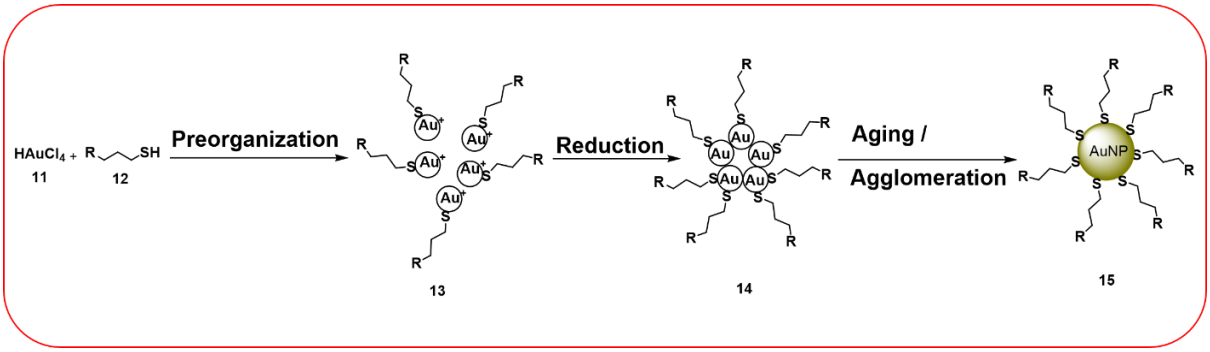

Scheme 1. Brust-Schiffrin technique for the formation of thiolated AuNps.[8]

2 Thiols on gold nanoparticles

2.1 Thermodynamics and kinetics of the Au-thiolate bond

The formation of a thiolate-gold bond first requires a chemical activation of the S-H bond of the thiol.[28,29] Seminal work by Dubois and coworkers have shown that Au-S bond strength can be quantified.[30,31] They studied the energetics involved in this bond activation, using temperature-programmed desorption experiment as a kinetic measure to determine the binding energy of the Au-S bond in a Surface Assembled Monolayer (SAM).[30,31] The result of this study showed that the adsorption of dimethyl disulfide (as a model compound) on Au(111) occurs dissociatively and the reaction is fully reversible, while the recombinative desorption of the sulfide is an activated process with a barrier close to 30 kcal·mol^{-1}.[30,31] Theoretical calculations have been used to back up this claim, and the results showed that for such a value to hold true, then a fairly significant degree of charge transfer must occur from the Au to the thiolates.[32] Moreover, using different experimental protocols, Scoles and co-workers also investigated the bonding energies of various organosulfur adsorbates on Au, and their studies suggest bonding energies close to 30 kcal·mol^{-1} for the case of SAMs, involving thiolated structures.[33] Other kinetic studies have revealed the complex nature of the Au-S bonding interactions. For instance, the groups of Whitesides and Liu, independently reported the results of desorption experiments that employed SAMs immersed in different solvents.[30,31,34] The kinetics of these processes can be modeled using conventional rate equations, and these models suggest barriers for the desorption process that are somewhat lower than the values obtained from desorption rate measurements made in Ultra High Vacuum (UHV) conditions.[30,31,34] In addition, Schlenoff and coworkers adopted a different approach and used electrochemical measurements to provide a detailed analysis of the Au-S bond energies, and desorption barriers for SAMs on gold.[35] Of particular interest was the estimation that the barrier for the bimolecular recombinative desorption of an alkylthiol from a SAM on gold, in the form of a dialkyl disulfide is 15 kcal·mol^{-1}.[35,36] This value is approximately a factor of 2 less than that deduced in the temperature-programmed desorption experiments. This discrepancy emanates from the fact that the measurement conditions are different, and thus, have different contributions from the heats of dissolution of the adsorbate and the heat of immersion of the substrate when immersed in an organic solvent.[36] In a nutshell, the analysis to be drawn from these differing

experiments is that, regardless of the different experimental conditions applied to study the Au-S bonding interaction, the Au-S bond is a very strong bond which obeys the Pearson's Hard and Soft Lewis acid and bases (HSAB) concept. This can further be rationalized with their frontier orbitals: the energy of the Highest Occupied Molecular Orbital (HOMO), of the thiol (a soft Lewis base), is higher and interacts with the Lowest Unoccupied Molecular Orbital (LUMO) of the soft Lewis acid, which has a lower energy, giving rise to strong bonds.[37]

2.2 Geometry of thiolated ligands on AuNps

NMR and IR experiments have shown that the geometry of thiols on AuNps is not far off from that on a 2D surface, indicating that these ligands adopt a linear geometry where they point vertically away from the Au surface.[29,38,39,40,41] However, an IR study of the structure of SAMs of alkylthiols on 1-2 nm gold clusters showed that the chain length can constitute some slight differences between planar SAMs and SAMs on Nps.[42] For all chain lengths, the SAMs on Nps exhibit a higher number of chain end-gauche defects than SAMs on planar surfaces.[42] The same study found that SAMs on Nps have a number of internal kink and near-surface defects similar to that of planar SAMs formed from alkylthiols of similar lengths.[42] (See Figure 4 and ref. 42 for further details).

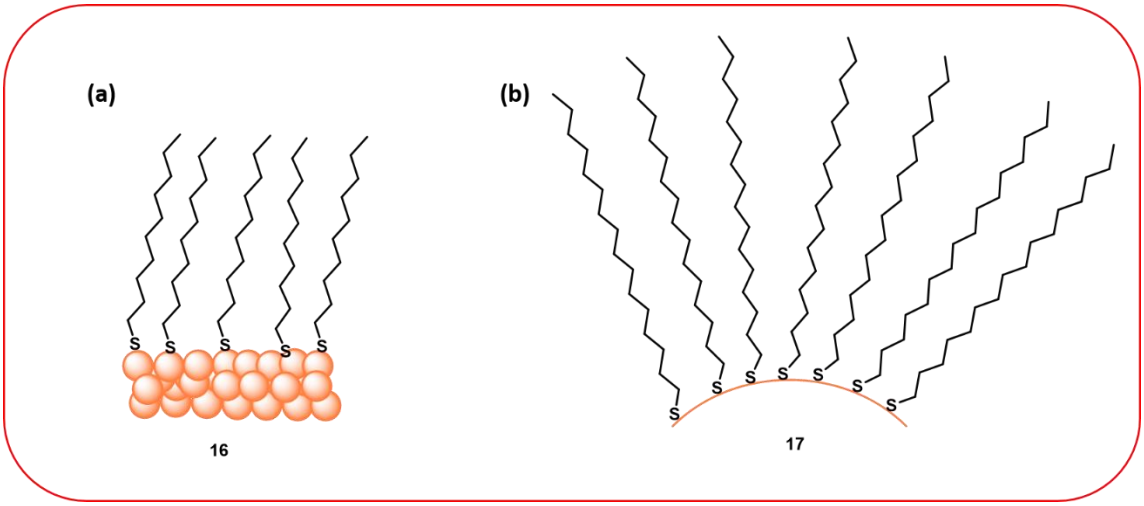

Figure 4. Schematic illustration of thiolated ligands on a) Au (111) surface[28] and b) AuNps.[38]

IR spectra of these Nps in CCl_4 showed a degree of disorder comparable to that of liquid alkanes.[41] One interpretation of the difference in IR spectra between solution and the solid phase is that the packing of the Nps in the solid state induces some degree of order on the alkylthiolates.[28] Alternatively, the solvation of the alkyl chains

by CCl_4 could account for the observed disorder.[28] Nevertheless, it is noteworthy to mention that, as the size of the Nps increases, the properties of the SAM tend to become more similar to an SAM on a planar surface.[28,40] For example, Nps with a core diameter greater than 4.4 nm, coated with an SAM of dodecanethiolates, have spectroscopic and physical properties which are comparable to that of a planar SAM.[28,40] While for 4.4 nm Nps, the majority of the surface comprises of flat (111) terraces rather than edges and corners.[28,40] This resulting geometry gives rise to bundles of ordered alkanethiolates with areas, having a disordered organic layer at the corners and vertexes, but still maintains a simple vertical geometry on the Au surface.[29,43] This adopted geometry is of vital importance in surface science, as it can be utilized to achieve selectivity in an organic on-surface synthesis.[1]

2.3 Influence of thiols on the sizes and shapes of AuNps

As described in the preceding section, the ratio of thiol to Au^{3+} salt, controls the size of the resulting Nps by adjusting the relative rates of particle nucleation and growth.[40,44] Methods of forming AuNps capped with thiolated ligands can only be used to form smaller–sized spherical AuNps.[45,46] The formation of Nps with diameters greater than 10 nm requires the use of different ligands that have a faster desorption rate than thiols such as phosphines and cetyltrimethylammonium bromide (CTAB).[45,46] Micrometer-sized Nps grown in the presence of an organic ligand that preferentially binds to a certain set of crystalline faces/facets will have a morphology that favors these facets.[47] The organic ligands act by lowering the free energy of the crystalline facets to which they bind and thereby, retard the growth of those facets.[13,28] These interactions control the resulting morphologies and sizes of crystals by selecting the crystalline planes that are expressed at the surface of the crystal.[13,28] The same principles may apply at the nanometer scale, where the differential binding of ligands to selected crystalline faces has been shown to influence the size, shape, and polymorph of nano materials.[48] Because of their decidedly non-bulk-like properties, thermodynamic arguments must be applied thoughtfully to nanoscale processes and particles.[49] Alkanethiols are not well-suited for controlling the shape of AuNps because thiols presumably have similar affinities for all crystalline faces.[50] It is this reason that AuNps formed in the presence of thiols usually adopt a roughly spherical shape.[50] On the other hand, metals with slightly more complex crystal structures than gold, equally have different crystalline faces with different surface energies that can bind to thiolated ligands with different

affinities. This differences make it possible to control the shape of the resulting Nps by either varying the ligand of choice or using a completely different metal precursor.[28,37]

3 *N*-Heterocyclic carbenes on gold nanoparticles

3.1 Introduction to *N*-Heterocyclic carbenes (NHC)

Carbenes contain a divalent carbon atom with a six-electron valence shell, and this incomplete electron octet has rendered free carbenes as highly reactive and short-lived intermediates in organic synthesis.[51] Due to its reactive nature, the isolation and unambiguous characterization of a free, uncoordinated carbene remained elusive until pioneering studies in the 20th century.[52] In 1988, Bertrand and co-workers proved that carbenes can be isolated and stabilized by favorable interactions with adjacent phosphorus and silicon substituents.[51,53,54] Three years later, Arduengo and co-workers followed similar trend and reported an isolable and storable carbene, incorporated into a nitrogen heterocycle.[53,54] Having a carbene incorporated into a heterocycle has opened up the usage of NHCs as excellent ligands for binding to the late transition metals and as such, their usage as both homogeneous and heterogeneous catalysts in chemical transformations.[29,55,56] There are several features or components of an NHC that impart its properties which in turn enable it to serve as a ligand for funtionalizing Au surfaces. Thus, the overall electronic and steric effects of these structural features go a long way to explaining the remarkable stability of the carbene carbon at the C^2 position (Figure 5). The wingtip position, adjacent to the C^2 position, could contain an aryl or alkyl substituent. Depending on the bulkiness of this substituent, it can help to kinetically stabilize the species by sterically disfavoring dimerization to the corresponding carbene dimer – a process known as the Wanzlick equilibrium (Scheme 2).[57]

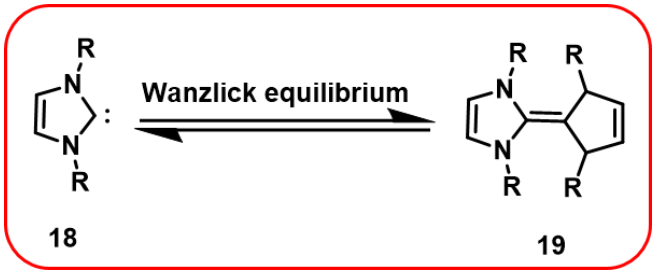

Scheme 2. Schematic representation of the Wanzlick equilibrium.

While the various substituents used at the backbone positions could be used to fine-tune the carbene electronics for the intended application while also imparting some stabilization by resonance – if this substituent is an aromatic moiety.[51]

On the other hand, the electronic stabilization provided by the nitrogen atoms (at the 1 and 3 positions) is however, a much more important factor. The adjacent σ-electron-withdrawing and π-electron-donating ability of these nitrogen atoms help to stabilize this structure both inductively (by lowering the energy of the occupied s-orbital) and mesomerically (by donating electron density into the empty p-orbital). This stabilization is necessary when one considers that, in addition to the obtainable triplet excited state configuration, these carbenes can also adopt a singlet ground-state electronic configuration with the LUMO and the HOMO which are best described as an unoccupied p-orbital at the C^2 carbon and the sp^2-hybridized lone pair, respectively (Figure 5). In addition, the cyclic nature of NHCs also helps to favour the singlet state by forcing the carbene carbon into a tilted or bent geometry, which is in harmony with sp^2-like hybridization. This ground-state structure is reflected in the C^2-N bond lengths of 1.37 Å, which fall in between those of its corresponding imidazolium salt of 1.33 Å and its C^2-saturated analogue of 1.49 Å, signifying that the C^2-N bonds are neither single nor complete double bonds, but possess partial double bond character.[53,54,58] Furthermore, the cyclic nature of the NHCs adds some substantial degree of stabilization just by virtue of its aromaticity, and this effect has been calculated to be around 25 kcal·mol^{-1} using imidazol-2-ylidenes as model substrates.[59]

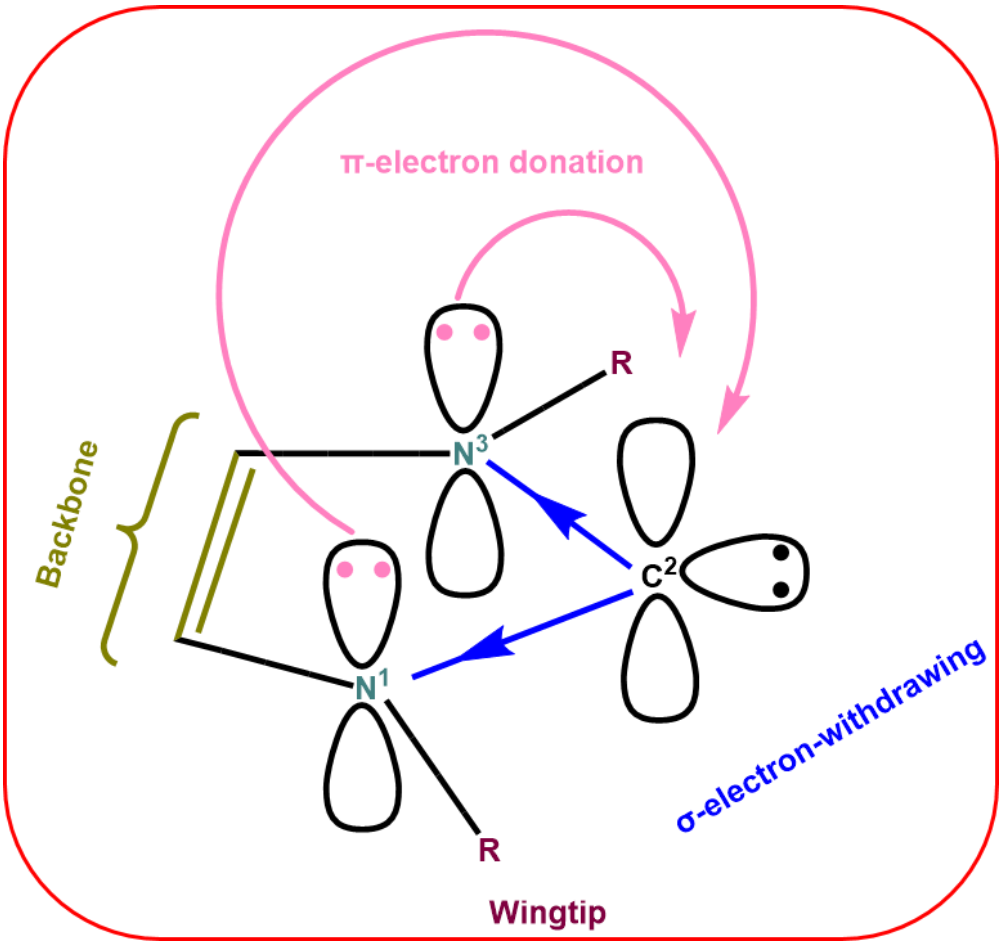

Figure 5. General representation of NHCs used in the stabilization of AuNps.[51,60]

3.2. NHC-Stabilized AuNps.

The first intentional use of NHCs as stabilizing ligands for Nps came independently from the groups of Fairlamb, Chechik and Tilley.[61,62] Chechik, Fairlamb, and co-workers described the preparation of NHC-functionalized AuNps by treating preformed dodecylsulfide-protected AuNps with free NHCs.[62] Incorporation of the NHC and loss of dodecylsulfide was confirmed by XPS analysis and these Nps were stable for long periods of time in the solid state.[62] However, in solution they were only stable for 12 h and subsequently degraded into $(NHC)_2Au^+$ and NHC-Au-X species, which were confirmed by NMR studies.[62] The Tilley group used a different approach to synthesize NHC-modified AuNps.[61,63] In this approach, the reduction of NHC−Au−Cl complexes with borohydrides or boranes gave rise to NHC coated AuNps.[61,63] The group of Tilley also observed an influence of the wingtip groups towards the Np synthesis: complexes with large wingtip groups did not result to the Nps, rather, they gave rise to molecular Au hydrides.[28,61] However, when treated with 1,3-diisopropylimidazol-2-ylidene, the complexes transformed into smaller-sized Nps which were difficult to purify.[28,61]

Nonetheless, employing complexes with long alkyl chains at the wingtip position under N_2 atmosphere, gave rise to NHC-protected AuNps that were stable for several months in the solid state and in solution, and were readily redispersible in a variety of solvents.[61] Therefore, the use of bottom-up synthesis (as in Tilley's approach), or top-down synthesis (as in Fairlamb and Chechik approach), nature of the starting Au^+ precursor, the reaction condition, as well as the nature of the reducing agent employed, will have a strong determining effect to the type of AuNps obtained from the synthesis.

3.3. Top-down syntheses of NHC-stabilized AuNps

The preparation of AuNps by top-down approach has been a popular method since it was first described in 2009 by Fairlamb and co-workers.[62] Subsequently, Richeter prepared NHC-stabilized AuNps by a top-down ligand exchange method starting from dodecylsulfide-protected Nps.[64] As is often the case in Np synthesis, concerns about the instability of the free carbene prompted its generation *in situ*, from the corresponding imidazolium salts along with a strong base.[64] Analogous to the work of Chechik and Fairlamb, Richeter observed precipitation of the Nps, which is likely due to the lack of stabilizing groups on the NHC.[64] In addition, significant quantities of molecular $(NHC)_2Au^+$ species were observed to contaminate the Nps, which may also be a consequence of solubility issues preventing efficient removal of molecular contaminants by washing.[64] Consistent with this result, the group observed that when NHCs, functionalized with long alkyl chains are used, then the resulting Nps were more soluble and the $(NHC)_2Au^+$ contaminant could be separated.[64] Their study did not only identify an important surface contaminant, but it also presented the first theoretical evidence for restructuring of the Au surface when bound to NHC ligand.[64]

NHC-protected Nps prepared via ligand exchange of thioether stabilized AuNps have also been reported by Glorius and coworkers.[65] In their study, methyl wingtip groups were employed in order to limit steric interactions with the surface of the Np, while the carbene and long alkyl chains were incorporated on the backbone of the carbene to inhibit sintering processes.[65] After reduction with *t*-BuONa to generate the free carbene, the solution was then exposed to an already pre-formed Np in a biphasic mixture of acetonitrile and hexane, to generate the desired functionalized Np in a ligand-exchange fashion.[65] Similarly, Yang, Chang, and co-workers described NHC-protected AuNps made using the ligand exchange method as catalysts for the electrochemical reduction of CO_2.[66] Ligand exchange was carried out on oleylamine-

stabilized AuNps employing the free carbene.[66] Solid-state ^{13}C NMR spectroscopy and Fourier Transform Infrared spectroscopy (FT-IR) were employed to confirm the ligand exchange and the obtained AuNps were further applied in the catalytic reduction of CO_2.[66] The AuNps showed enhanced catalytic activity for CO_2 reduction compared to bare AuNps along with improved Faradaic efficiency, making these species interesting for electrocatalysis.[66] In summary, each functionalized AuNp is designed for a specific purpose and this purpose will determine the choice of its synthetic route.

3.4. Bottom-up syntheses of NHC-Stabilized AuNp.

Pileni and Roland have described numerous examples of NHC-stabilized AuNps, synthesized by bottom-up approaches.[67–70] In their first report, a bottom-up approach was employed by reduction of various NHC−Au−Cl complexes.[67,68] In one of their early approaches, thiolated ligands were added alongside the NHC ligand with the aim of targeting an improved stability.[68] However, the same group later reported that this method is not viable, but leads to Nps whose surfaces are predominantly covered with thiols, rather than NHCs (with a reported 10% NHC surface coverage as determined from XPS).[67] However, the reduction of Au complexes without an additional thiol gave NHC-protected AuNps, which were shown to have considerably higher stability in solution as well as under the highly oxidative environment of oxygen plasma.[67] In addition, Pileni and Roland have reported the self-assembly of AuNps bearing long alkyl chains into 3D super lattices by the controlled evaporation of colloidal solutions of the Nps.[70] Ultrasmall AuNps were prepared by Guari, Monge, and co-workers by thermal decomposition of NHC-ligated Au complexes.[71] Various methods were employed to prepare these AuNps, which involved subjection to high temperatures of 250 and 285 °C to produce ultrasmall AuNps.[71] Analysis of the Nps by MALDI-TOF gave peaks which suggest that the NHC still remained on the AuNps after thermal decomposition and somehow, managed to be catalytically active for the reduction of 4-nitrophenol with $NaBH_4$.[71]

Lee, Song, and co-workers utilized NHCs functionalized with bis-thiophene moieties at the wingtip groups to prepare the Au complex.[72] When the chloride ligand was removed from these complexes with AgOTf, simultaneous polymerization of the bis-thiophene units occurred, with an accompanying Np formation.[72] The authors proposed that the cationic Au^+ complexes disproportionated to Au^0 and Au^{3+} complexes, with the Au^{3+} species mediating the polymerization of the bis-thiophene

units and the Au^0 species decomposing to generate the Nps.[72] While these Nps were not of the best quality, they were however, superior to those created without the NHC present, which underwent rapid aggregation.[72] In a similar bottom-up fashion, Crudden and Nazemi described the use of amphiphilic NHC ligands for AuNps where one wingtip group contained a long alkyl chain and the other had a triethylene glycol group.[73] The NHC−Au−Br complexes were reduced with $NaBH_4$ in a biphasic solvent system of water and dichloromethane (DCM) to yield highly uniform-sized AuNps, which were further purified by dialysis.[73] The self-assembly of these AuNps was carried out in polar solvents such as deionized water and ethanol, which was employed to preferentially solubilize the groups at the wingtip position.[73] While some small aggregates were observed in water, much larger, higher aggregates were observed in ethanol, which was confirmed by a shift in the SPR from 525 to 555 and 580 nm, respectively, for water and ethanol solutions.[73] This corroborated the fact that the dispersing medium can also influence the size and properties of the AuNps just as described in the preceding section.

Crudden and coworkers reported the first example of the use of ditopic NHC ligands for the stabilization of AuNps using both the bottom-up and top-down methods and compared the stability of the resulting Nps from these two different methods.[74] The influence of both denticity and the absence or presence of long alkyl chains on the backbone of the NHC was also examined.[74] For the top-down approach, Nps protected with dodecyl sulfide were used as starting materials, and the bidentate NHCs were introduced as the free carbenes.[74] TEM analysis showed that the resulting Nps were of similar sizes as the starting Nps, indicating that little to no etching took place during the reaction.[74] However, in the bottom-up approach, preformed NHC-Au-X complexes were reduced with $NaBH_4$ in ethanol, yielding NHC-stabilized AuNps that were approximately 2 nm in diameter.[74] The bottom-up method gave rise to smaller-sized AuNps when compared to the top-down method with the same ligand.[74] All the AuNps prepared with this ditopic NHC ligand (which do not have long alkyl chains), aggregated in solution within 1 week.[74] By comparison, Nps protected with alkylated NHCs showed a very high thermal stability even up to 130 °C, but it is noteworthy to mention that a variation in sizes was observed afterwards, via the SPR band.[74] In addition, thiol-degradation studies illustrated that the method of preparation was more paramount than the ligand denticity.[74] Thus, NHC-stabilized AuNps, with long alkyl chains, prepared via the top-down approach were more stable than similar NHCs

prepared via bottom-up approach.[74] Similarly, Toste and co-workers reduced NHC−Au−Cl complex with boranes and borohydride and were further stabilized by incorporation within a dendrimer to prevent the sintering of the AuNps.[75] This stabilization resulted in an increase of catalytic activity for lactonization at 20 °C versus the ligandless AuNps, which were inactive below 80 °C for this reaction.[75]

These two above-described reports showed how different parameters within the same or different synthetic routes (Scheme 3), and the presence or absence of surface ligands could influence the outcome and reactivity of the obtained Np.

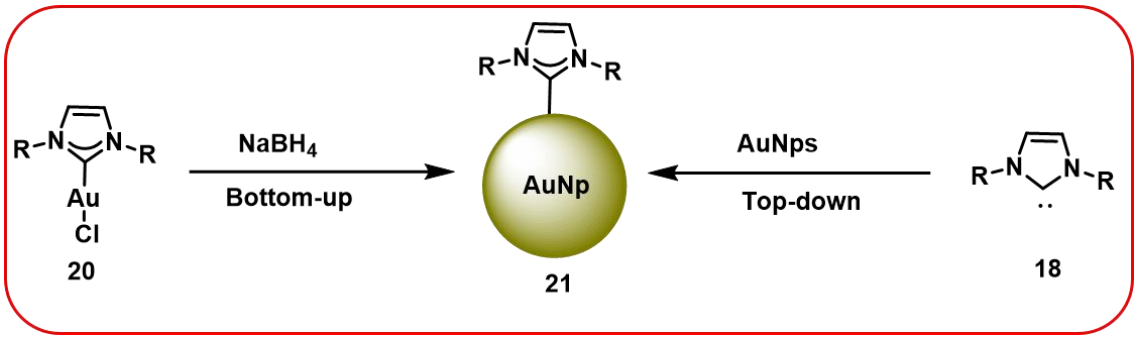

Scheme 3. Bottom-up and top-down syntheses of NHC-functionalized AuNps.[76]

3.5. Geometry of NHCs on Au surfaces

The Au-NHC bond strength is 2.8 times stronger than that of Au-S bond and thus, estimated at 82.8 kcal·mol^{-1}.[77,78] This difference in bonding strength also gives rise to differences in bonding geometry, stability, chemical reactivity and an overall application of AuNps functionalized with NHC ligands.[51,55,73,78,79] The binding geometries of NHCs to flat gold surfaces have been intensively studied using near-edge X-ray absorption fine-structure spectroscopy (NEXAFS),[80] scanning tunneling microscopy (STM),[81,82] and high-resolution electron-energy loss spectroscopy(HREELS).[81] Crudden and co-workers first demonstrated the wingtip dependent orientation of NHCs on Au(111) surface.[78,81] They observed that NHCs with sterically bulky wingtips display a tendency to form upright configurations while NHCs with less bulky wingtip groups primarily form flat-laying species.[78,81] In a similar fashion, Glorius, and other authors have also investigated the effects of wingtip size on the binding motif of the NHC on Au(111) surface, and observed that NHCs with smaller wingtips can additionally form dimer structures that attach to the surface via an adatom.[81–83,84] However, the usage of NEXAFS, STM and HREELS is only limited to 2D surfaces and not applicable to 3D AuNps. For this reason, Camden and coworkers adopted SERS to determine the absolute configuration of NHCs on 3D AuNps.[85] The result of this study is shown in

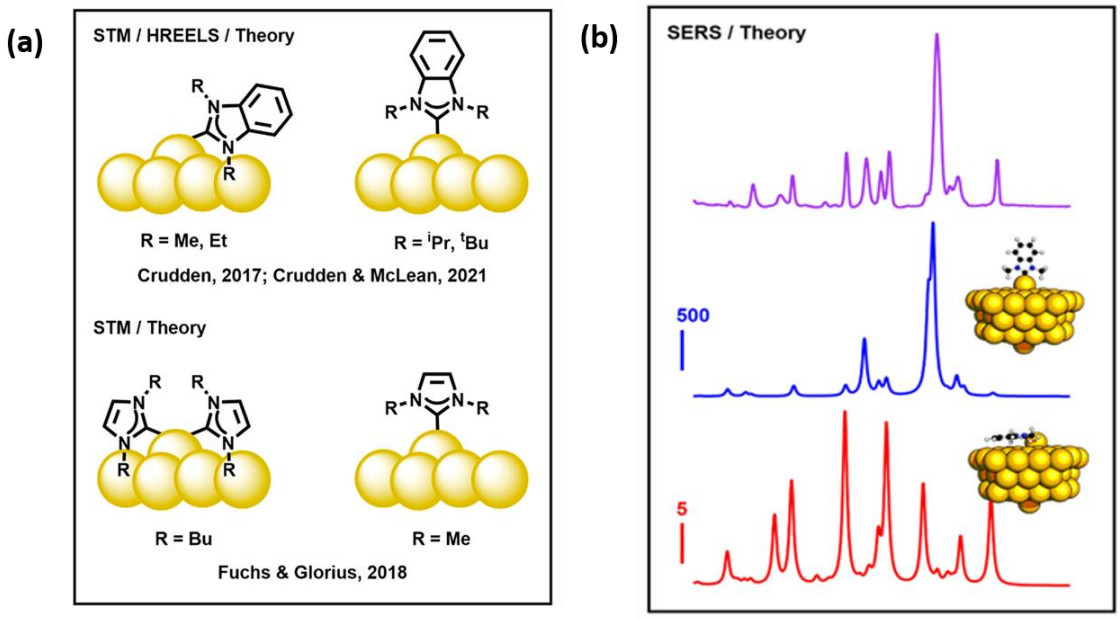

Figure 6. Geometries of NHC ligands on a) 2D Au surface and b) 3D spherical AuNps indicating that both the vertical and flat geometries are obtainable on 3D AuNps, Reproduced with permission from ref.[85] Copyright © 2023, American Chemical Society.

Figure 6, which proves that both configurations are obtained on the surface of AuNps.[85] The NHC ligands adopt both the flat and upright configurations in which they abstract a Au adatom and ride on it in a ballbot-type motion, across the surface of the AuNp.[85] This is also in accordance with the reports of Glorius and coworkers.[83,86] The fascinating results obtained from the in-depth studies of geometry of NHCs on Au surfaces, led to the application of NHCs as suitable surface ligands for conducting organic reactions on 2D surfaces. A term known as organic on-surface synthesis, and this concept will be explained in detail in the succeeding chapter.

4 Organic On-surface Synthesis

During the last decade, traditional in-solution (homogeneous catalysis), and gas-phase synthesis (heterogeneous catalysis) have been extended to single crystal surfaces in UHV environment, which is commonly termed as Organic On-surface synthesis.[87–89,90,91–98] With the help of STM and AFM, the molecular structures, properties of the reactants and those of the final products can be characterized with better atomic resolution.[87,91–97] More importantly, high reactive intermediate states with transient lifetimes can be stabilized by surfaces at low temperatures and captured with STM and AFM, providing a deeper insight on the reaction mechanisms occurring on these defined surfaces.[87,88,99] Tireless efforts have been made to control the on-surface reaction pathways as well as their outcomes.[88,89,100] The influences of the chemical structures of the precursors and the underlying surfaces to the on-surface reactions have also been scrutinized.[88,89,100] It has been proved that in most cases, the mono or bilayer surfaces do not only serve as reaction catalysts but can as well serve as important supports that mediate the reactions.[97,101] The versatility of this technique has been proven and applied in diverse organic reactions such as Ullmann reactions,[86,101] dimerization of NHCs,[102] condensation reactions of boronic acids,[103] imine formation,[104] acylation reactions,[105] Bergman cyclization,[106] cyclodehydrogenation,[107] click reactions,[108] and cycloaddition reactions.[109] However, given the scope of this work, more emphasis will be placed in the on-surface Ullmann reactions.

4.1 On-surface Ullmann coupling

The generally accepted mechanism for the Ullmann reaction involves multiple steps including: formation of an organometallic intermediate from a molecule containing an aryl halide, an oxidative addition with another molecule, and a reductive elimination to furnish the final product.[110] However, the actual intermediate is still under debate. In the surface-confined Ullmann reaction, different intermediates have been proposed.[111,112] For example, the working groups of Xi, Bent and Blake proposed that 1,4-iodobenzene molecules form a protopolymer on Cu(111) that features a surface-mediated interaction between dehalogenated phenyl moieties and the surface atoms.[87,91,98,113] The same surface-mediated structures were observed by Lipton-Duffin[111] using Cu(110) and was later evidenced by Lewis and coworkers on cobalt

islands.[114] Nevertheless, Walch and coworkers reported a different intermediate structure formed by a larger polyphenyl molecule on Cu(111) and Ag(111), but followed the same above-described mechanism.[115] Based on intermolecular distances resolved in STM topographs, the authors proposed that the intermediate is an aryl−metal−aryl coordination complex in which the metal atom is an adatom that sits on the same plane as the aryl moieties.[115] Similar structure has also been reported in an anthracene moiety adsorbed on a Ag surface.[116] Several other mechanistic insights have been gained towards on-surface reactivities. For example, Wang and coworkers have characterized the reactants, intermediates, and products obtained from the Ullmann coupling reaction of terphenyl moieties on Cu(111) (Figure 7a).[117] Using STM and Density Functional Theory (DFT) modeling, they showed that the intermediate structure, which forms at an intermediate temperature, consists of large, bright ovals and small, dimdots in a periodic chain arrangement (Figures 7b,c).[117] The dots are the Cu adatoms while the ovals are terphenyl moieties. Figure 7c showed that the Cu atoms lie nearly coplanar with the terphenyl moieties and that each Cu atom formed two C−Cu bonds (where C−Cu = 2.11 Å) with the neighboring terphenyl units.[117] The tunneling spectra (Figure 7d) showed that the terphenyl moieties featured a prominent peak at +1.7 V, whereas the Cu atom featured a gradually rising intensity.[117] The calculated projected density of states (PDOS) of the terphenyl moiety showed a sharp peak at +2.7 V, while the Cu adatom had no apparent features.[117] The calculated PDOS was in fair agreement with the experimental tunneling spectra. The inset in Figure 7c showed a simulated STM image of the intermediate structure at +2.7 V, and mimicked the main features of the experimental STM image. The intermediate structure was found to convert to the final products of polyphenylene chains at 470 K.[117] Similarly, Chen and coworkers studied the adsorption and reaction of functionalized benzene units on Cu(111) surface using XPS.[118] The molecules were vapor deposited onto Cu(111) at a sample temperature of 170 K.[118] Br 3p and C 1s X-ray photoelectron spectra were taken at 170 K and at higher temperatures.[118] At 170 K (Figure 7f), the Br $3p_{3/2}$ signal consisted of a single peak at 184.1 eV, which was associated with intact functionalized benzene moieties.[118] Once the sample was heated to 240 K, the original Br $3p_{3/2}$ peak at 184.1 eV was almost fully converted into a peak at 182.4 eV.[118] No significant changes were observed after heating to higher temperatures of up to 473 K, indicating that the C−Br bond scission was complete at 240 K.[118] A single C 1s peak appeared at 285 eV, as shown in Figure 7g. This peak

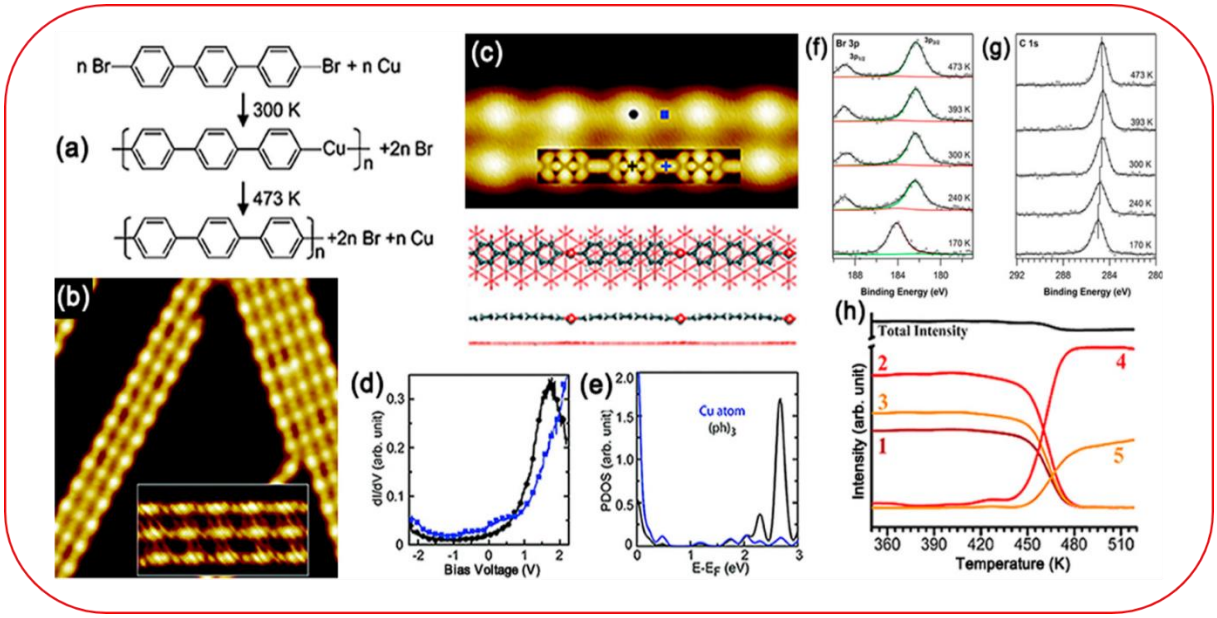

Figure 7. Mechanism for on-surface Ullmann coupling reactions. (a) The pathway of on-surface Ullmann coupling of terphenyl moieties on Cu(111). (b) STM image of the sample annealed at 300 K (20 × 20 nm^2). Inset: Br atoms lying between the linear structures (8 × 4 nm^2). (c) High-resolution STM image of the intermediate (8 × 4 nm^2) and the DFT-calculated structure. Inset: DFT-simulated STM image at +2.7 V. (d) dI/dV spectra measured at terphenyl (black) and Cu (blue)marked in panel c. (e) Calculated PDOS of Cu (blue) and terphenyl (black). Reproduced with permission from ref.[119]Copyright © 2015, American Chemical Society (f) Br 3p and (g) C 1s XP spectra of functionalized benzene units on Cu(111) with a coverage of θ = 0.027 (around 0.9 monolayers). Functionalized benzene moieties were deposited on Cu(111) with the substrate held at 170 K. Reproduced with permission from ref.[119] Copyright © 2015, American Chemical Society (h) Intensity functions of C 1s core levels as a function of annealing temperature acquired by fast-XPS measurement. One is assigned to carbon bound to copper, 2 and 3 are assigned to the dehalogenated phenyl molecules, and 4 and 5 are assigned to the coupled carbon. Reproduced with permission from ref.[119]Copyright © 2015, American Chemical Society

shifted gradually to a lower binding energy upon increasing temperatures, up to 393 K. From 393 to 473 K, the peak shifted back to higher binding energy.[118] Di Giovannantonio and coworkers used fast-XPS to monitor the dynamic transition from an organometallic intermediate structure to covalently bonded polymers.[88] They demonstrated how temperature controlled the evolution of the organometallic intermediate in Ullmann coupling of 1,4-dibromobenzene on a Cu(110) surface.[88] Spectral analysis confirmed that debromination was complete at room temperature and the C 1s core level peak at 283.2 eV was assigned to C−Cu binding, supporting the proposition that an organometallic intermediate incorporating C−Cu bonds, forms at room temperature.[88] Analysis of the peak intensities of the C 1s state as a function of annealing temperature (Figure 7h) suggested that the vanishing of the peak at 283.2 eV could be considered the limiting step for the conversion into covalent bond.[88] All these reports demonstrate that the on-surface Ullmann reaction follows the

formation of an organometallic intermediate via an oxidative addition, with a subsequent reductive elimination that gives rise to the formation of a C-C covalent bond.

Nevertheless, notwithstanding the fascinating advantages on-surface synthesis has to offer with regards to reaction selectivities and synthesis of new and/or elusive organic architectures, it is still limited to 2D flat surfaces and UHV conditions. This flat surface is an essential criterion for visualization of reaction products using AFM, and in most cases, limits the use of CO-functionalized tip of an AFM. In other words, this technique is limited to single molecules and not suitable for the bulk material synthesis obtained from in-solution organic syntheses. All these demerits led to the idea of developing new ways of conducting organic reactions, which were successfully achieved in the course of this work. In this developed technique, we were able to show for the first time, that chemical reactivities can be transferred from a 2D surface which requires UHV conditions, to a 3D Au-surface in solution, which does not require UHV condition. We also showed that the new geometry adopted by the reactants when attached to a 3D Au-surface, can be used to attain reaction selectivities, similar to that obtained on a 2D surface. Furthermore, we went ahead to establish the general parameters that govern when these reactions on 3D surfaces will be successful and when they will be unsuccessful. Simply put, the feasibility and failure of this reaction can now be predicted. Thus, aiding a reproducibility of this new method for future work in molecular self assembly, nanotechnology and in organic synthesis. All these discoveries will be discussed in detail in the following section and sub-sections.

5 Contributions to literature

5.1 Ullmann coupling reactions on Gold Nanoparticles

Reference: N. Ukah, H. A. Wegner, *Chem. Eur.* **2024**, e202400024.

DOI: 10.1002/ceur.202400024

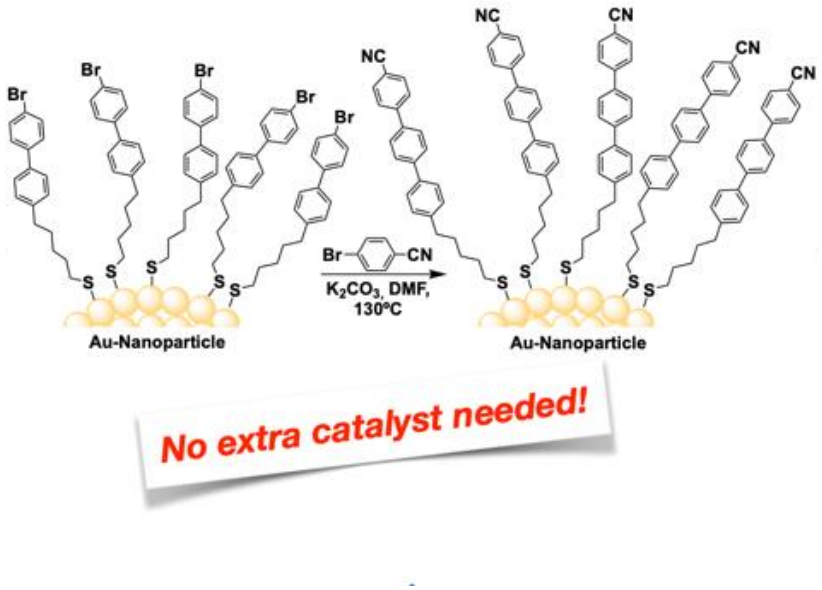

''There has been a plethora of experience in conducting organic reactions in solution, with little to no knowledge in organic reactions on surfaces. Broadening the horizon of organic on-surface synthesis will enable creation of functional materials and direct integration into devices. Herein, we report an Ullmann reaction on thiol-functionalized gold nanoparticles serving as reactant, stabilizing agent, catalyst and reducing agent in this transformation. The orientation of ligands and formation of Surface Assembled Monolayer (SAM) on the gold nanoparticles were exploited to attain selectivity of hetero- over homo-Ullmann coupling, thus, expanding the toolbox of organic on-surface synthesis to nanoparticles''.

Check for updates
ChemistryEurope
Excellence in Chemistry Research Worldwide

Research Article
doi.org/10.1002/ceur.202400024

www.journal.chemistry-europe.org

Ullmann Coupling Reactions on Gold Nanoparticles

Nathaniel Ukah[a, b] and Hermann A. Wegner*[a, b]

There has been a plethora of experience in conducting organic reactions in solution, with little to no knowledge in organic reactions on surfaces. Broadening the horizon of organic on-surface synthesis will enable creation of functional materials and direct integration into devices. Herein, we report an Ullmann reaction on thiol-functionalized gold nanoparticles serving as reactant, stabilizing agent, catalyst and reducing agent in this transformation. The orientation of ligands and formation of Surface Assembled Monolayer (SAM) on the gold nanoparticles were exploited to attain selectivity of hetero- over homo-Ullmann coupling, thus, expanding the toolbox of organic on-surface synthesis to nanoparticles.

Introduction

The Ullmann reaction has been established as an efficient method to construct nanostructures directly on surfaces.[1-3] This arises from the fact, that it enables C—C bond formations in situations where there are one or more of the same or different aryl halides, without the need for an additional organometallic species. Besides its widespread use in both in-solution-based and on-surface syntheses, it has been posed with many disadvantages, such as poor functional group tolerance, harsh reaction conditions, longer reaction times, low product yields and poor selectivity towards hetero-coupled products.[4] Most of these aforementioned demerits have been solved using appropriate ligands and catalysts via in-solution chemistry, with the exception of clear selectivity between the homo- and the hetero-coupled product.[4-6] In some cases, the former reaction tends to be faster than the latter, resulting to an appreciable yield of the homo-coupled product in Ullmann reactions. On the contrary, on-surface syntheses have proven that this issue of selectivity in Ullmann reactions can be surmounted using molecule-by-molecule manipulations just as predicted by the Feynman model.[1,3] Previous work have shown that, adsorbing coupling partners to a 2-D Au(111) surface will enable these molecules to be oriented in a manner that they can be dehalogenated using voltage pulse and subsequently dragged and dropped, using a CO-functionalized tip of an Atomic Force Microscope (AFM).[1-3] With this technique, organic molecules which remained elusive by in-solution synthesis became selectively accessible by on-surface synthesis. Nevertheless, this method is limited to single molecules and not suitable for bulk material synthesis. Because, reaction products are primarily determined by the number of available radicals that could be brought to proximity using a CO-functionalized tip of an AFM, thus, giving rise to limited quantities of covalent architectures on a 2-D surface.[3] Additionally, these protocols are conducted in ultrahigh vacuum (UHV) conditions, which in turn, require stringent measures that limit the the use of high molecular weight precursors as starting materials.

In a quest to attain bulk materials in Ullmann reactions in a selective manner, we devised a protocol for Ullmann coupling reactions on organic-inorganic hybrid materials using thiol-functionalized gold nanoparticles (AuNps). Furthermore, the method enables access to nanoparticles functionalized with a covalent organic network cover, opening a new area of materials. Such an organic-inorganic hybrid material consists of a core, the shell, a binding group, an organic linker, and a reaction partner (Scheme 1). The core of the hybrid material houses the majority of the Au atoms existing in the zero (0) oxidation states. The shell comprises of the surface atoms of the AuNps. These surface atoms have lower coordination than the core atoms, giving rise to free sites with non-bonded orbitals, which allow interaction with ligands, preventing Np agglomerations.[7,8] In the simplest form, binding to the Np surface involves the transfer or exchange of electrons between a surface atom and the ligand binding group.[9] We chose thiol functionalized ligands because the strong Au—S covalent bond offers a robust protection of AuNps for long-term stability, while being relatively weak enough to enable increased reactivity on the surface of these nanoparticles as opposed to very strong binding carbenes.[10] The linker acts to separate and/or provide distance between the AuNp and the aromatic moiety. The linker can also be used to effectively tune the distance and in some cases, the energy transfer to the AuNp thus, reducing steric influences that can arise from directly connecting the binding group to the reaction partner.[11-14] These linkers are usually chemically inert, such as alkyl chains,[14,15] phenyl units,[12-14] triazole rings,[16] ethers[14] or amides.[17] However, a linker should be long enough to minimize electronic and steric effects between the AuNps and the aromatic moiety. We thereby, settled for a pentyl chain as a linker, since it is chemically and

[a] N. Ukah, Prof. Dr. H. A. Wegner
Institute of Organic Chemistry
Justus Liebig University Giessen
Heinrich-Buff-Ring 17, 35392 Giessen (Germany)
E-mail: Hermann.A.Wegner@org.chemie.uni-giessen.de

[b] N. Ukah, Prof. Dr. H. A. Wegner
Center for Materials research (ZfM/LaMa)
Justus Liebig University Giessen
Heinrich-Buff-Ring 16, 35392 Giessen (Germany)

Supporting information for this article is available on the WWW under https://doi.org/10.1002/ceur.202400024

ChemistryEurope
Excellence in Chemistry Research Worldwide

Research Article
doi.org/10.1002/ceur.202400024

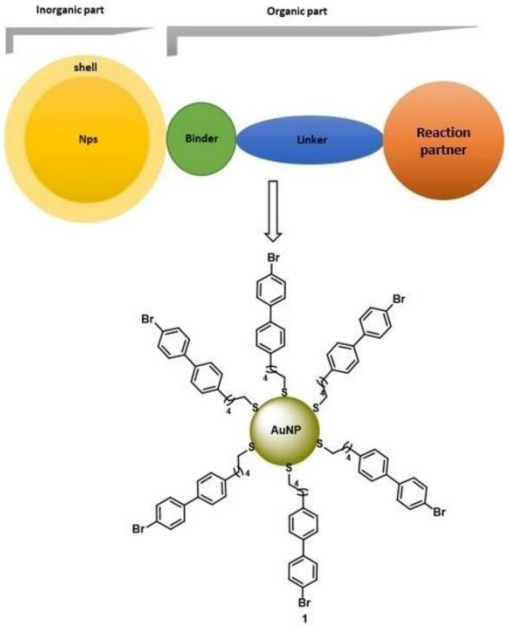

Scheme 1. Schematic representation of an organic-inorganic hybrid material.

optically inert and in turn, provides suitable distance between the AuNps and the aromatic moiety. The reaction partner could be an aromatic molecule, which was functionalized with a halogen group to enable coupling reaction on the surface of AuNps. We used a biphenyl molecule due to its similarity to our previous on-surface studies.[1-3] Putting all these described elements together, we arrived at **1** as a model system for our on-surface functionalization. Therefore, our organic-inorganic hybrid material serves as a reducing agent (that is, the core), as a catalyst (the shell), a stabilizing agent (binder and linker) and as reactant (reaction partner) for Ullmann coupling reactions (Scheme 1).

Results and Discussion

Synthesis and characterization of thiol-functionalized AuNps: The Synthesis of target compound **1**, was done from **2**, which is commercially available. Lithiation of **2** with *n*BuLi at -78 °C followed by the introduction of **3** furnished the intermediate in 46 % yield (Scheme 2). The intermediate was reacted with thiourea by refluxing in EtOH for 5 h, followed by a one-pot basic quench with NaOH to eliminate urea as a side-product while furnishing **5** in 60 % yield. There are several methods for functionalizing thiols with AuNps. We applied a modified Brust- Schiffrin technique in synthesizing the thiol functionalized AuNps, since this technique enables the obtained AuNps to be precipitated and further re-dispersed in solution, which is suitable for further on-surface functionalizations.[6,18,19] This aforementioned protocol furnished the as-prepared AuNps which were thoroughly washed with EtOH to remove unbound alkyl-aryl thiols. The thiol-functionalized AuNps were characterized with H-NMR spectroscopy, Transmission Electron Microscopy (TEM), Dynamic Light Scattering (DLS), Thermogravimetric Analysis (TGA), UV-Vis and X-ray Photoelectron Spectroscopy (XPS).

^{1}H-NMR spectroscopy was applied to ascertain the purity of the prepared nanoparticles and to follow-up the direct attachment of thiols to the surface of the AuNps (Figure 1). The results showed a complete disappearance of the signals corresponding to C_1 protons next to the thiol group followed by broadenings of C_2 and C_3 protons. For other protons, there were slight changes in the chemical shift values with significant broadening relative to the free thiol. The variation in chemical shift is due to the structural change of capping groups and proximity to the surface of the nanoparticles, in which the ligand forms Au—S with gold atoms on the shell. This predominantly affects the C_1 and C_2 protons. The NMR resonance broadenings are primarily due to different chemical environment arising from the formation of Surface Assembled Monolayer around the AuNps. This phenomenon is a function of the sizes as well as the

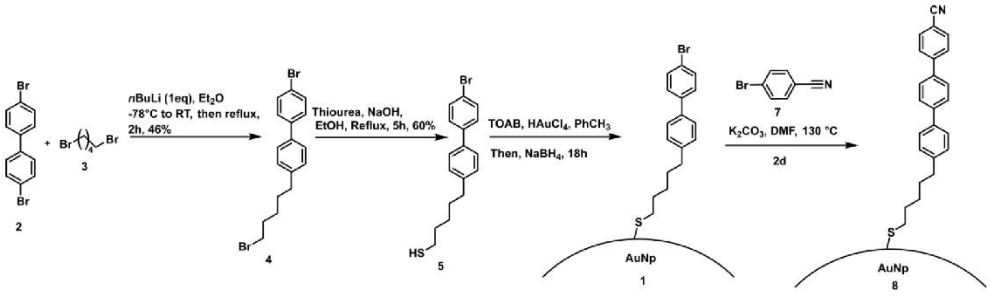

Scheme 2. Syntheses of thiol-functionalized AuNps **2**-**8**.

ChemistryEurope
Excellence in Chemistry Research Worldwide

Research Article
doi.org/10.1002/ceur.202400024

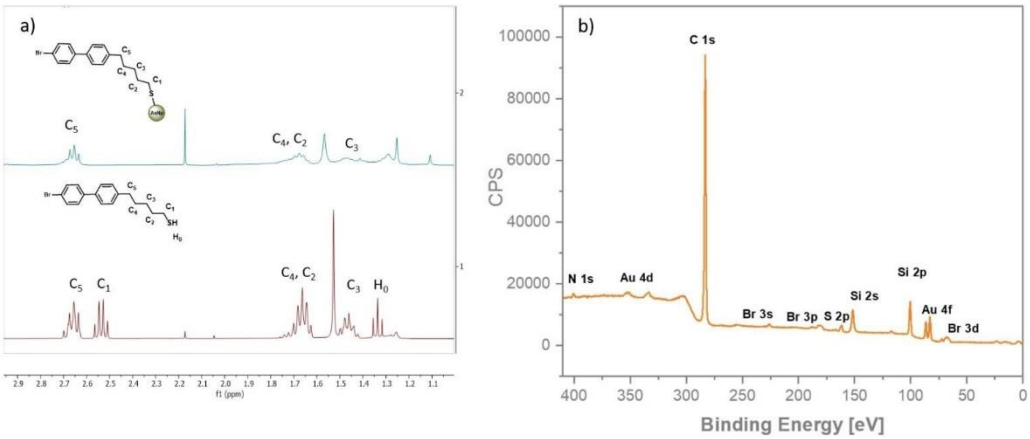

Figure 1. Analysis of alkyl aryl thiols as a Surface Assembled Monolayer on AuNps; a) H NMR of thiol ligand **5** and thiol-functionalised AuNps **1** and b) XPS spectrum of thiol-functionalized AuNp **1**.

transversal interproton dipolar relaxation mechanism that is rendered more efficient by the restricted rotational mobility of the ligands when bound to the surface of the AuNp.[20] TEM was carried out to determine the sizes and morphologies of the thiol-functionalized AuNps. The result showed that the nanoparticles have a well-defined spherical shape with an average diameter of 6.70 ± 1.59 nm (Figure S1). This value is also similar to other AuNps synthesized using the Brust-Schiffrin approach.[22] However, DLS measures both the core sizes of the AuNps, the ligands attached to the core of the AuNps as well as the solvent cage generated by the nanoparticles. In principle, the sizes obtained from DLS are usually larger than that obtained from TEM. Therefore, the thiol-functionalized AuNps showed a hydrodynamic diameter of 19 nm and a zeta potential of 0.144 mV suggesting a neutrally charged AuNp (see Supporting Information, Figure S3). There were no multiple distribution peaks observed from the DLS spectrum, which suggests a uniformity in hydrodynamic size and internal structure of the functionalized AuNps. Furthermore, TG analysis of the functionalized AuNps revealed the presence of thiol and AuNp in the ratio of 67 : 33, indicating a successful incorporation of the ligands to the Au shell (see Supporting Information, Figure S5). Combining the results obtained from TGA with that obtained from TEM analysis, we were able to compute the number of thiolated ligands on each AuNp using the technique adopted in literature.[23] An average number of 11400 alkyl aryl thiols was found to be present on each Np. This result confirmed that we successfully synthesized bulk materials as opposed to single molecules obtained by Ebeling and co-workers using a 2-D Au(111) surface.[3] Furthermore, a comparison of the UV-Vis absorption spectra of **1** with the starting material **2**, showed a uniform band at 255 nm which is predominantly due to the $\pi \rightarrow \pi^*$ transition of the biphenyl moiety. Nonetheless, there was no Surface Plasmon Resonance (SPR) band of gold at 530 nm, which is a function of sizes of the AuNps as well as ligand of functionalization.[10] In smaller-sized hybrid materials, there is a strong quantum confinement of electrons in this size regime, the electron energy quantization occurs, and this effect drastically alters the physical and chemical properties of metal Nps, such as an increase in the band gap.[10,18] This phenomenon gave rise to a blueshift of the SPR band in the UV-Vis spectrum (Figure S6). In addition, SPR band of noble metal nanoparticles is a function of refractive index, and any slight change of refractive index, arising from the direct attachment of surface ligands could result to a complete disappearance of an SPR band.[10,25] Conversely, we used X-ray Photoelectron Spectrsocopy (XPS) to confirm the presence of Au in the synthesized Np. XPS spectrum of **1** showed a doublet at 85 eV corresponding to Au4f$_{7/2}$ orbital and this value is in perfect agreement with that reported in literature for AuNps.[19,20] Combining the results from H NMR spectroscopy, TGA, UV-Vis and XPS, we conclude that small, spherical, thiol-functionalized AuNps **1** were successfully synthesized.

Reaction on the Surface of AuNps

We envisaged that the arrangement of the alkyl aryl thiols as a Surface Assembled Monolayer (SAM) on the AuNps, will prevent a homo-Ullmann reaction between the ligands on the same AuNp due to lack of proximity between the bromine atoms. On the other hand, the SAM will enable a high degree of selectivity towards hetero-Ullmann coupling of an introduced coupling partner with the ligands on the AuNp. To support our proposition, we carried out a hetero-Ullmann reaction of **1** with **7** under conventional Ullmann conditions[6] and monitored the product of the reaction using ATR-IR spectroscopy. Figure 2a

ChemistryEurope
Excellence in Chemistry Research Worldwide

Research Article
doi.org/10.1002/ceur.202400024

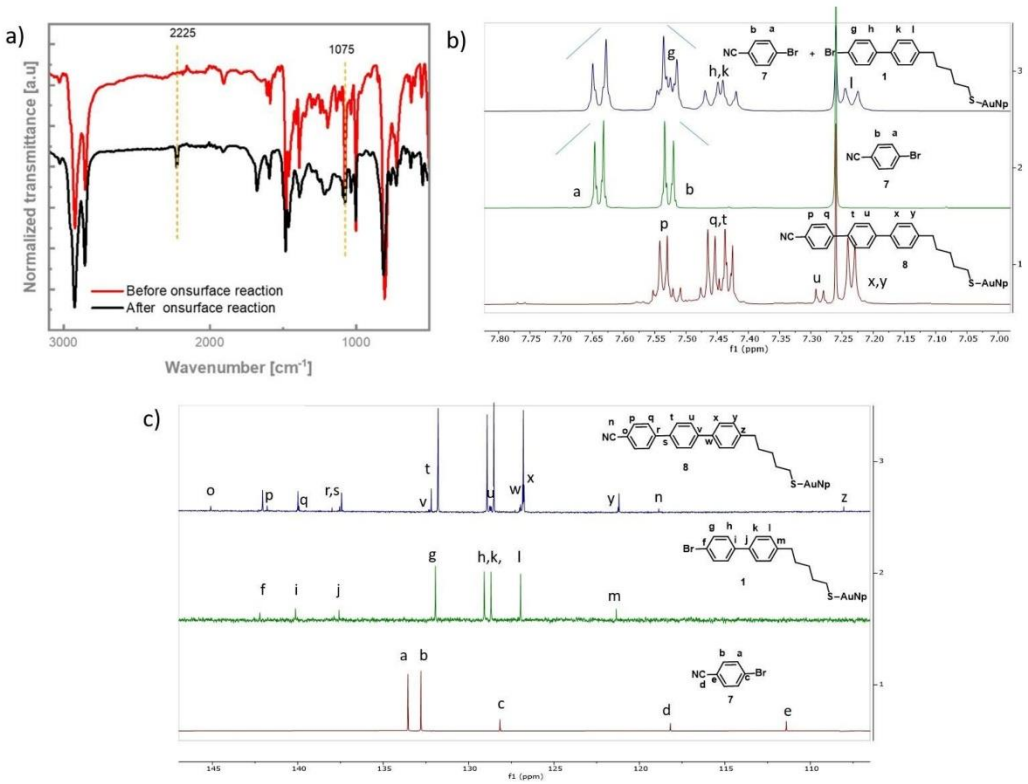

Figure 2. Proof of on-surface functionalization. a) ATR-IR spectra of thiol-functionalized AuNps before and after on-surface reaction. b) H-NMR spectra of a physical mixture of **1** and **7** (top spectrum), *p*-bromobenzonitrile (middle spectrum) and coupled product on the AuNp (bottom spectrum). c) ^{13}C-NMR spectra of of **8** (top spectrum), unreacted AuNp, **1** (middle spectrum) and **7** (bottom spectrum).

showed a reduction of the band at 1075 cm^{-1} which is assigned to the aromatic C—Br vibration, indicating that some of the aromatic C—Br bonds have been replaced by a C—C bond. In addition, there was an appearance of a band at 2225 cm^{-1} which was invisible in the functionalized AuNps before reaction (Figure 2a). This band corresponds to the CN vibration introduced as a nitrile group on the terphenyl moiety. The rest of the spectrum was unperturbed, indicating the functionalized AuNp was only modified at the bromine position. To prove that the band at 2225 cm^{-1} is coming from the coupled product on the AuNp and not due to some unreacted *p*-bromobenzonitrile - which also has a CN functionality. We thereby, prepared a mixture of both starting materials, that is, **1** and **7**, in the mass ratio of 1 : 3 (as determined from TG analysis and used during the reaction), and measured the H-NMR of this mixture. The spectrum was compared to that of the coupled product on the AuNp, alongside the spectrum of **7**. Figure 2b showed the AB spin system of *para*-substituted aromatics with J_{AB} of 1.1 Hz, corresponding to *p*-bromobenzonitrile. This spin system was also observed in the NMR spectrum of a physical mixture of **1** and **7** but was absent in the spectrum of **8**. This observation validates the assertion that the coupled product on the AuNp is not a physical mixture of the both starting materials.

We employed the sensitivity of proton decoupled ^{13}C-NMR spectroscopy to molecules in complex mixtures, to monitor the introduced functional group as a terphenyl ring on the surface of the AuNps. ^{13}C-NMR spectra showed proofs of hetero-Ullmann reaction with additional signals at 118.9 ppm and 145.1 ppm, which could be unambiguosly assigned to carbons at *alpha* and *beta* positions to the nitrile group. These values are also in perfect agreement with that reported in literature.[21] On the other hand, ^{13}C-NMR showed retention of signals corresponding to the starting material, compound **1**. This indicates that the reaction did not attain 100 % conversion but exists as a mixed monolayer comprising of both the coupled ligands and the uncoupled ligands attached to the same Np (Figure 2c). The surface functionalization was finally confirmed with Secondary Ion Mass Spectrometry (SIMS). Analysis of the

ChemistryEurope
Excellence in Chemistry Research Worldwide

Research Article
doi.org/10.1002/ceur.202400024

secondary ion beam showed an m/z peak at 357.1620 which is congruent to the mass of **8** (Figure S7). Therefore, SIMS result underpins the results obtained from ATR-IR, H- and C-NMR spectroscopy, which suggest a formation of a heterocoupled product on the surface of the AuNps. To further confirm that there is a chemical reaction on the surface of the functionalized AuNps, we modified the coupling partner from *p*-bromobenzonitrile to *p*-bromo-trifluorotoluene, performed the same Ullmann coupling and monitored the reaction using ^{19}F NMR spectroscopy. Compound **9** was chosen as a substitute for **7** as both CN and CF_3 groups have a resonance-electron withdrawing effect on aromatic rings and should thereby, show similar reactivity. The results from the ^{19}F-NMR spectra displayed three peaks, at -62.80, -62.70 and -62.40 ppm which could be particularly assigned to **9**, homocoupled product of **9**, and **10** respectively (Figure S8).[24] This corroborates the results of ATR-IR and ^{13}C NMR indicating that there is a chemical reaction on the surface of the AuNps, other than a physical trapping of **7** in the cavity of the thiol functionalized AuNps. To demonstrate that the formation of SAM enables selectivity for heterocoupling reaction with no possibility for a homo-Ullmann coupling, we carried out a test reaction with **1** while maintaining the same reaction conditions used for the heterocoupling. After 2d of reaction time at 130 °C, there was no evidence for a homocoupled product, other than an increase in the diameter of the AuNps when exposed to higher temperatures of the reaction. This result could be explained from lack of proximity of these ligands to each other when attached to the surface of the AuNps. Furthermore, to prove that the coupling reaction was mediated by the AuNps directly attached to the sulfur of the alkyl aryl groups, we conducted two different test reactions with separate mixtures of **4** and **7** and **5** and **7**. These two mixtures were subjected to the same reaction conditions used for the reaction of **1** and **7**. After 2d of reaction time at 130 °C, there was no evidence for neither homo-coupling or heterocoupling reaction. This observations confirmed the fact that Au specie is needed either in the form of nanoparticle or Au complex to mediate an oxidative addition, followed by a reductive elimination that furnishes the coupled product as a newly formed C—C bond.[4-6]

Nonetheless, it is noteworthy to mention that the functionalized AuNps are stable at 130 °C and still exist as nanoparticles at the temperature of reaction. XPS spectrum of the reacted nanoparticles showed signals at 283, 161 and 82 eV, corresponding to C 1s, S 2p and Au 4f orbitals, indicating a retention of the AuNps with the attached ligands on the surface of the Nps (Figure S9). Additionally, there were XPS signals at 236 and 182 eV corresponding to Br 3s and Br 3p orbitals, thus, underscoring the result of ^{13}C-NMR which suggests the presence of unreacted starting material (that is, compound **1**), and the coupled product (compound **8**), attached to the same surface and existing as a mixed monolayer on the surface of the AuNp. Furthermore, DLS spectrum of **8** showed multiple distribution peaks with increased hydrodynamic diameters at 1, 3 and 276 nm which suggests a polydispersity of the AuNps after on-surface reaction. In addition, a small zeta potential of 0.231 mV was obtained for compound **8** which is indicative of a neutral AuNp, and a tendency of flocculation when dispersed in solution. Similarly, TEM showed an increase in core sizes of the Nps with an average core size of 50.5 ± 29.7 nm (Figure S12). These two observations indicate aggregation phenonema at higher temperatures of reaction, but with a retention of the nanoparticles after on-surface reaction.

Conclusions

In conclusion, we synthesized alkyl aryl thiols and functionalized them with AuNps using a modified approach of the Brust-Schiffrin technique. The formation of SAM on the surface of AuNps was confirmed with H NMR, TEM, DLS, TGA, UV-Vis and XPS. We utilized the orientation of the ligands generated by the formation of SAM to attain selectivity of hetero- over homo-Ullmann coupling which otherwise, would have been difficult to achieve via in-solution organic synthesis. Ullmann reactions on these AuNps were characterized with a combination of ATR-IR, H NMR, ^{19}F NMR, ^{13}C NMR and SIMS. Spectroscopic studies with XPS, DLS and TEM showed that the hybrid material still exists as a nanoparticle after undergoing a selective hetero-Ullmann reaction, thus, opening new prospects in organic on-surface synthesis to a new class of organic-metal hybrid materials.

Experimental Section

Synthesis of 4: *n*-Butyllithium (10.7 mL, 1.00 eq, 17.2 mmol) was slowly added to 4,4-dibromobiphenyl (5.48 g, 1.00 eq, 17.2 mmol) in anhydrous diethylether (172 mL) at −78 °C under nitrogen. Subsequently, 1,5-dibromopentane (15.8 g, 4.00 eq, 68.8 mmol) was slowly added to the reaction mixture at -78 °C under nitrogen. The mixture was warmed up to rt and then stirred at reflux. After 2h of reflux, the reaction mixture was cooled down to rt and quenched by adding cold water (17.2 mL). The crude mixture was extracted with diethylether (3×34 mL) and the combined extracts were washed with saturated NaCl solution (3×34 mL), dried over $NaSO_4$ and concentrated under reduced pressure to give the crude product. The obtained solid was purified by column chromatog- raphy using cyclohexane and EtOAc (10 : 1) as eluent, followed by a second column chromatography using pure cyclohexane to give 2.76 g (15.7 mmol, 46 %) of pure alkyl aryl dibromide product as a colourless waxy solid.

^1H NMR (400 MHz, $CDCl_3$): δ = 7.56-7.53 (m, 2H), 7.48-7.43 (m, 4H), 7.24-7.26 (m, 2H), 3.42 (t, *J* = 6.8 Hz, 2H), 2.67 (t, *J* = 7.4 Hz, 2H), 1.91 (m, 2H), 1.68 (m, 2H), 1.53 (m, 2H). ^{13}C NMR (101 MHz, $CDCl_3$): δ = 141.74, 140.99, 139.83, 138.44, 137.35, 131.64, 128.54, 126.73, 35.18, 33.61, 32.54, 30.43, 27.67. HR-MS (APCI): m/z calcd for $C_{17}H_{18}Br_2$: 379.9775, found: 380.9853 $(M+H)^+$.

Synthesis of 5: The alkyl aryl bromide **4** (1.09 g, 1.00 eq, 2.85 mmol) and thiourea (2.17 g, 10.0 eq, 28.5 mmol) were dissolved in ethanol (37 mL) and refluxed for 3 h under nitrogen. An aqueous solution of degassed sodium hydroxide (11.4 mL, 10.0 eq, 2.50 M) was added to the reaction mixture and was refluxed for another 2 h under nitrogen. The reaction mixture was cooled down to rt. 1 M HCl was added to adjust the pH to 5 and the mixture was extracted with DCM (3×25 mL). The combined extracts were washed with saturated NaCl solution (2×25 mL), and dried over anhydrous Na_2SO_4. The organic layer was concentrated and purified by column

ChemistryEurope
Excellence in Chemistry Research Worldwide

Research Article
doi.org/10.1002/ceur.202400024

chromatography over silica gel with pure cyclohexane as an eluent to obtain 0.570 g (2.85 mmol, 60 %) of the product as a colorless waxy solid.

^{1}H NMR (400 MHz, $CDCl_3$): δ = 7.55-7.54 (m, 2H), 7.48-7.44 (m, 4H), 7.26-7.24 (m, 2H), 2.67 (t, J = 7.47 Hz, 2H), 2.55 (q, 7.44 Hz, 2H), 1.68 (m, 4H), 1.48 (m, 2H), 1.35 (t, J = 7.74 Hz, 1H). ^{13}C NMR (101 MHz, $CDCl_3$): δ = 141.92, 139.85, 137.28, 131.64, 128.78, 128.40, 126.66, 121.05, 35.25, 33.72, 30.69, 28.90, 24.38. HR-MS (APCI): m/z calcd for $C_{17}H_{19}BrS$: 334.0391, found: 334.0335 (M^+).

Synthesis of Thiol-Functionalised AuNps

The flasks were precleaned with Aqua regia, water and acetone and dried at 120 °C, to remove any residue metal contaminants. $HAuCl_4$ (0.0136 g, 1.00 eq, 0.0400 mmol) in 5.00 ml HPLC water and tetraoctylammonium bromide (TOAB) (0.0262 g, 1.20 eq, 0.0480 mmol) in 10.0 ml toluene were combined in a 25 ml tri-neck round bottom flask. The solution was vigorously stirred at rt for 15 min at 1100 rpm, and the aqueous layer was then removed with 10 mL syringe. Compound **5** (0.0536 g, 4.00 eq, 0.160 mmol) was added to the flask, and stirring was reduced to a very low speed (50 rpm). After 2 h of stirring at rt, the stirring speed was increased to 1100 rpm, and immediately $NaBH_4$ (0.0156 g, 10.0 eq, 0.400 mmol) in 5.00 ml HPLC water was rapidly added all at once. After 24 h of rapid stirring at rt, the aqueous part was removed, dried in vacuum at 50 °C and was thoroughly washed with ethanol to obtain the thiol functionalized AuNps.[6,18]

General Procedure for on-Surface Functionalization

The flasks were precleaned with Aqua regia, water and acetone and dried at 120 °C, to remove any residue metal contaminants. Under typical Ullmann conditions, functionalized AuNp (**1**) (40.0 mg), K_2CO_3 (34.8 mg), and 4-bromobenzonitrile (**7**) (3.86 mg) were mixed in 0.500 ml DMF and stirred at 130 °C under N_2 for 2 d. The reaction propagation was monitored by TLC analysis. The reaction mixture was diluted with excess H_2O and extracted with DCM. The organic layer was successively washed with water (3×20 mL) and dried over anhydrous $MgSO_4$. The solvent was evaporated under reduced pressure and the product was separated by Gel Permeation Chromatography, with HPLC chloroform as an eluent to obtain **8** as a golden-yellow sticky solid.

General information, NMR spectra of all compounds, TEM, DLS, TGA, XPS and UV-Vis spectra are provided in the Supporting document.

Acknowledgements

The authors wish to express their sincere gratitude to Sebastian Benz and David Schäfer for the XPS and SIMS measurements respectively. In addition, the authors acknowledge the financial support provided by the LOEWE Program of Excellence of the Federal State of Hesse (LOEWE Focus Group PriOSS 'Principles of On-Surface Synthesis') and Justus Liebig University.

Conflict of Interests

The authors declare no conflict of interest.

Data Availability Statement

The data that support the findings of this study are available in the supplementary material of this article.

Keywords: Surface chemistry · C—C coupling · Surface analysis · Gold · Nanoparticles · S-ligands

[1] D. Ebeling, Q. Zhong, T. Schlöder, J. Tschakert, P. Henkel, S. Ahles, L. Chi, D. Mollenhauer, H. A. Wegner, A. Schirmeisen, *ACS Nano* **2019**, *13*, 324-336.
[2] J. Tschakert, Q. Zhong, D. Martin-Jimenez, J. Carracedo-Cosme, C. Romero-Muñiz, P. Henkel, T. Schlöder, S. Ahles, D. Mollenhauer, H. A. Wegner, et al., *Nat. Commun.* **2020**, *11*, 5630.
[3] Q. Zhong, A. Ihle, S. Ahles, H. A. Wegner, A. Schirmeisen, D. Ebeling, *Nat. Chem.* **2021**, *13*, 1133.
[4] L. Wang, W. Lu, *Org. Lett.* **2009**, *11*, 1079.
[5] Y.-C. Yeh, B. Creran, V. M. Rotello, *Nanoscale* **2012**, *4*, 1871.
[6] G. Li, C. Liu, Y. Lei, R. Jin, *Chem. Commun.* **2012**, *48*, 12005.
[7] D. A. Hines, P. V. Kamat, *ACS Appl. Mater. Interfaces* **2014**, *6*, 3041.
[8] L. M. Rossi, J. L. Fiorio, M. A. S. Garcia, C. P. Ferraz, *Dalton Trans.* **2018**, *47*, 5889.
[9] J. de Roo, M. Ibáñez, P. Geiregat, G. Nedelcu, W. Walravens, J. Maes, J. C. Martins, I. van Driessche, M. V. Kovalenko, Z. Hens, *ACS Nano* **2016**, *10*, 2071.
[10] M. W. Brett, C. K. Gordon, J. Hardy, N. J. L. K. Davis, *ACS Phys. Chem. Au.* **2022**, *2*, 364.
[11] N. Tripathi, M. Ando, T. Akai, K. Kamada, *ACS Appl. Nano Mater.* **2021**, *4*, 9680.
[12] Z. Huang, M. L. Tang, *J. Am. Chem. Soc.* **2017**, *139*, 9412.
[13] Z. Huang, Z. Xu, T. Huang, V. Gray, K. Moth-Poulsen, T. Lian, M. L. Tang, *J. Am. Chem. Soc.* **2020**, *142*, 17581.
[14] X. Li, Z. Huang, R. Zavala, M. L. Tang, *J. Phys. Chem. Lett.* **2016**, *7*, 1955.
[15] V. Gray, Z. Zhang, S. Dowland, J. R. Allardice, A. M. Alvertis, J. Xiao, N. C. Greenham, J. E. Anthony, A. Rao, *J. Phys. Chem. Lett.* **2020**, *11*, 7239.
[16] A. Rossi, M. B. Price, J. Hardy, J. Gorman, T. W. Schmidt, N. J. L. K. Davis, *J. Phys. Chem. C* **2020**, *124*, 3306.
[17] C. Xia, W. Wang, L. Du, F. T. Rabouw, D. van den J. Heuvel, H. C. Gerritsen, H. Mattoussi, C. de Mello Donega, *J. Phys. Chem. C* **2020**, *124*, 1717.
[18] M. Zhu, E. Lanni, N. Garg, M. E. Bier, R. Jin, *J. Am. Chem. Soc.* **2008**, *130*, 1138.
[19] J. F. DeJesus, L. M. Sherman, D. J. Yohannan, J. C. Becca, S. L. Strausser, L. F. P. Karger, L. Jensen, D. M. Jenkins, J. P. Camden, *Angew. Chem. Int. Ed.* **2020**, *59*, 7585.
[20] Z. Hens, J. C. Martins, *Chem. Mater.* **2013**, *25*, 1211.
[21] N. Ballav, B. Schüpbach, O. Dethloff, P. Feulner, A. Terfort, M. Zharnikov, *JACS* **2007**, *129*, 15416.
[22] A. Manna, P.L Chen, H. Akiyama, T.X Wei, K. Tamada, W. Knoll, *Chem. Mater.* **2003**, *15*(1), 20-28.
[23] M. J. MacLeod, J. A. Johnson, *J. Am. Chem. Soc.* **2015**, *137*, 7974-7977.
[24] F. Izquierdo, M. Corpet, S. P. Nolan, *EurJOC* **2015**, *2015*, 1920.
[25] R. A. M. Lameirinhas, J. P. N. Torres, A. Baptista, M. J. M. Martins, *IEEE Photonics J.* **2022**, *14*, 1.

Version of record online: ■■, ■

RESEARCH ARTICLE

Expanding organic on-surface synthesis enables functional material creation and device integration. Herein, an Ullmann reaction on thiol-functionalized gold nanoparticles is presented, which act as reactant, stabilizer, catalyst, and reducing agent. Ligand orientation by Surface Assembled Monolayer (SAM) formation on nanoparticles enhances selectivity for hetero-Ullmann coupling, advancing nanoparticle-based organic synthesis.

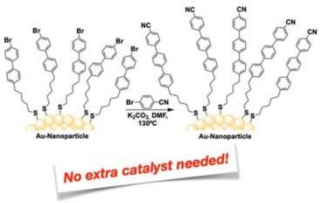

*N. Ukah, Prof. Dr. H. A. Wegner**

5.2 On-Surface Synthesis - Ullmann coupling reactions on *N*-Heterocyclic Carbene functionalized gold nanoparticles

Reference: N. Ukah, H. A. Wegner, *Nanoscale* **2024**.

DOI: 10.1039/D4NR03065F

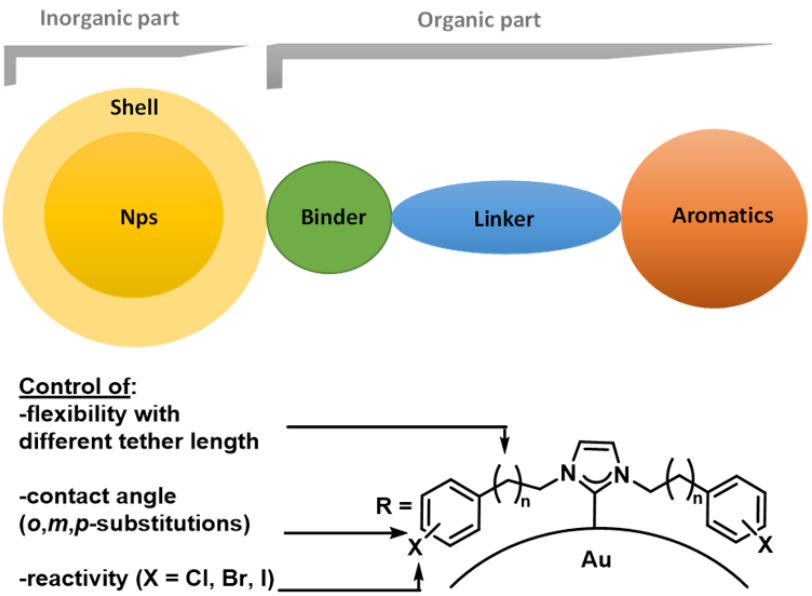

‘’Organic on-surface syntheses promise to be a useful tool for direct integration of organic molecules onto 2-dimensional (2D) flat surfaces. In the past years, there has been an increasing understanding about the mechanistic details of reactions on surfaces, however, mostly under ultra-high vacuum on very defined surfaces. Herein, we expand the scope to gold nanoparticles (AuNps) in solution via an Ullmann reaction of aryl halides connected via *N*-heterocyclic carbenes (NHCs) to AuNps. Through design and syntheses of various organic precursors, we addressed the influence of the contact angle, reactivity of the halogen and the proximity of the entire coupling partner towards on-surface reactivities, thus, establishing general parameters governing organic on-surface syntheses on AuNps in solution, in comparison to the reactivity on defined surfaces under ultra-high vacuum. The retention of such halogenated Nps at higher temperatures of reaction holds great promise in the fields of material engineering, nanotechnology and molecular self assembly, while expanding the toolbox of organic chemistry synthesis in accessing various covalent architectures’’.

ARTICLE

Received 00th January 20xx,
Accepted 00th January 20xx

DOI: 10.1039/x0xx00000x

On-Surface Synthesis - Ullmann coupling reactions on N-Heterocyclic Carbene functionalized gold nanoparticles

Nathaniel Ukah,*[a,b] and Hermann A. Wegner[a,b]

Organic on-surface syntheses promise to be a useful tool for direct integration of organic molecules onto 2-dimensional (2D) flat surfaces. In the past years, there has been an increasing understanding about the mechanistic details of reactions on surfaces, however, mostly under ultra-high vacuum on very defined surfaces. Herein, we expand the scope to gold nanoparticles (AuNps) in solution via an Ullmann reaction of aryl halides connected via *N*-heterocyclic carbenes (NHCs) to AuNps. Through design and syntheses of various organic precursors, we addressed the influence of the contact angle, reactivity of the halogen and the proximity of the entire coupling partner towards on-surface reactivities, thus, establishing general parameters governing organic on-surface syntheses on AuNps in solution, in comparison to the reactivity on defined surfaces under ultra-high vacuum. The retention of such halogenated Nps at higher temperatures of reaction holds great promise in the fields of material engineering, nanotechnology and molecular self assembly, while expanding the toolbox of organic chemistry synthesis in accessing various covalent architectures.

Introduction

The idea of confining reactions to a flat substrate has led to the transition of a chemical environment from a typical three-dimensional reaction space in solution phase to a seemingly two-dimensional platform.[1–21] This new environment has the potential to facilitate alternative reaction pathways to those available in solution, giving rise to new selectivities and intermediates which are otherwise difficult to obtain via in-solution organic synthesis.[1–9,12,14,19] A prototype of this molecule-by-molecule manipulation, is the work of Ebeling and coworkers,[22] who attained a high degree of selectivity between the homo- and hetero-coupling of aryl halides by adsorbing the reaction partners to a 2D Au(111) surface followed by dehalogenation with voltage pulses. The generated radicals were dragged and dropped, using a CO-functionalized tip of an Atomic Force Microscope (AFM), to provide organic structures which are difficult to access via in-solution synthesis.[22] Similarly, the group of Glorius[23] synthesized and deposited *N*-heterocyclic carbenes (NHCs) on crystalline gold surfaces in high vacuum and performed an Ullmann coupling of these moieties to obtain covalently linked ballbot-type repeating units of NHCs, bound to single Au ad-atoms. A combination of scanning tunnelling microscopy (STM), non-contact AFM, X-ray photoelectron spectroscopy (XPS) and density functional theory (DFT) calculations were used to determine the conformational properties, steric influence, binding mode, electronic properties, and the surface alignments of these new covalent architectures.[23] Nevertheless, these aforementioned techniques require organic precursors to be deposited under ultra-high vacuum (UHV) conditions and onto highly defined single crystalline flat surfaces. Only then visualization with AFM is possible. That way, only single molecules are produced and as such, not suitable for syntheses of larger, isolatable amounts of material. With the option to attain bulk materials in Ullmann reactions in a selective manner, we moved from defined planar surfaces in high vacuum to nanoparticles in solution, and devised a protocol for Ullmann coupling reactions using NHC-functionalized gold nanoparticles (AuNps) as reaction platform. Our system offers advantages compared to the system of Glorius,[23] such as: (1) it avoids sublimation of molecules to the surface allowing high molecular weight precursors as starting materials. This fact allows expanding the scope of on-surface reactivities to different varieties of organic materials. (2) It extends the availability of products from single molecules to larger amounts of material, since reaction products are no longer limited by the amount of radicals being dragged and dropped using the tip of an AFM. (3) It expands the concept on-surface synthesis to organo-halogen-functionalized nanoparticles, whose prospects range from molecular self assembly[24,25] to enhancement of X-ray Computed Tomography (CT) scans.[26] In general, the technique delivers Nps functionalized with a new covalent organic network cover, which is a new class of organic materials. In addition, we aimed to transfer parameters that control on-surface syntheses on highly controlled surfaces under high vacuum, to Np in solution. Furthermore, we investigated parameters

[a] Institute of Organic Chemistry
Justus Liebig University Giessen
Heinrich-Buff-Ring 17, 35392 Giessen (Germany)
E-mail: Hermann.A.Wegner@org.chemie.uni-giessen.de
[b] Center for Materials research (ZfM/LaMa)
Justus Liebig University Giessen
Heinrich-Buff-Ring 16, 35392 Giessen (Germany).
†Electronic Supplementary Information(ESI) available:See
DOI: 10.1039/x0xx00000x

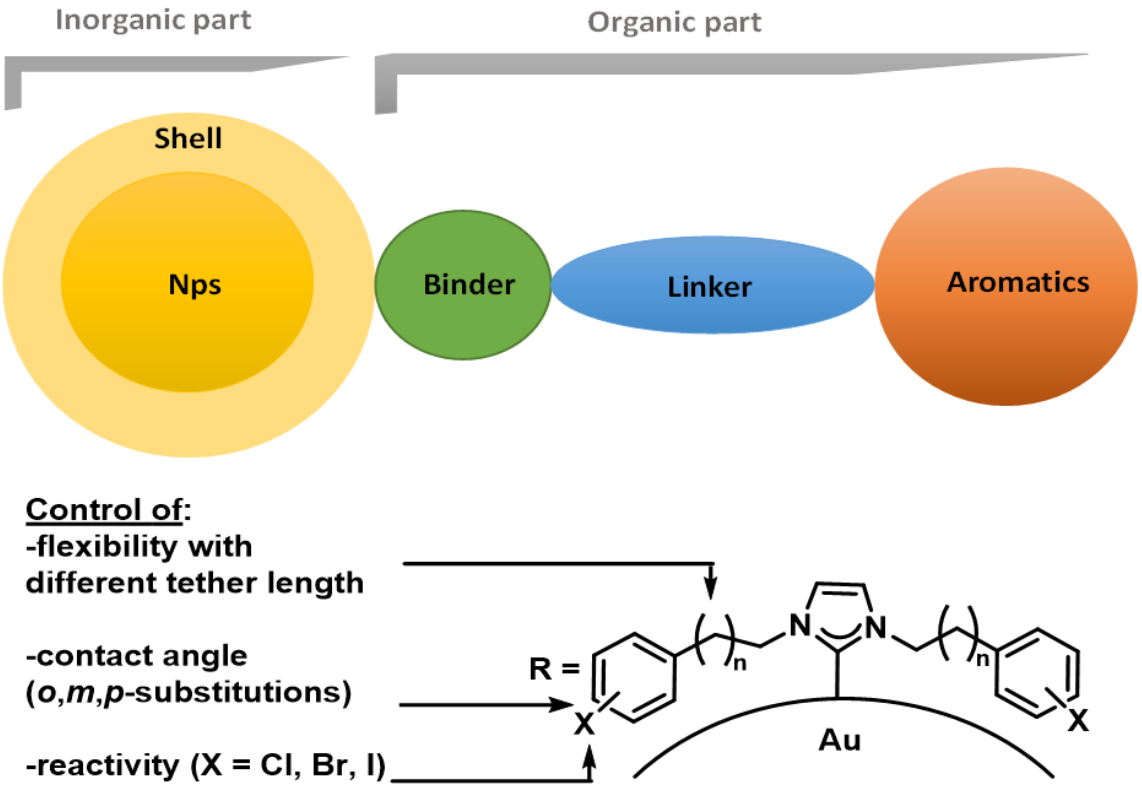

Scheme 1 Schematic representation of the organic-inorganic hybrid material and the different parameters studied in this work.

that control on-surface syntheses, by a systematic variation of the NHC-coupling precursor, for example, determining the effect of contact angle of the hybrid material through positioning the halogen in *ortho*, *meta* and *para* positions, probing the effect of the tether length towards on-surface Ullmann coupling reactions and exploiting the different reactivity of aryl chlorides, bromides and iodides towards on-surface functionalizations. The devised organic-inorganic hybrid material studied in this work, consists of a core, the shell, a binding group, an organic linker, and a reaction partner (Scheme 1). The core of the hybrid material comprises majority of Au atoms in the oxidation state zero (0). The shell consists of the Au-surface atoms and are direct bound to the organic ligand, in the present case a σ (carbene) electron-donating group.[27] As the orbitals of the metal interact with the ligands, metal-metal interaction are reduced.[27,28] This metal-ligand interaction enhances stabilization and prevents Np agglomerations.[27,29,30,31] We chose carbenes as organic ligands due to its strong binding to the AuNps similar to the previous system reported by the group of Glorius.[23] More importantly, the tilted geometry of carbenes enables the groups at the wingtip positions to point towards the surface of the Np resulting to an increased proximity of the reacting partners to the surface of the AuNps.[1,3,9,21,32] Therefore, variation of the binding group allows to altering the geometry, and hence, the chemical reactivity of the hybrid material. That way, for example, the selectivity of either inter- or intramolecular Ullmann reactions should be controlable. The linker part of the organic ligand separates the AuNp from the aromatic moiety and can be used to effectively tune the distance between the AuNp and the aromatic group.[33–35] Finally, an aryl halide was chosen as the reaction partner for the Ullmann-coupling reaction of the hybrid material, which was functionalized at a suitable position. Putting all these described elements together, **1f-AuNp** was designed as a model system for our on-Np-surface functionalization (Scheme 2). In this case, the organic-inorganic hybrid material performs the function of a catalyst (the AuNp), stabilizing agent (the NHC) and of reactant (reaction partner at the wingtip positions) in the investigated Ullmann coupling reactions.

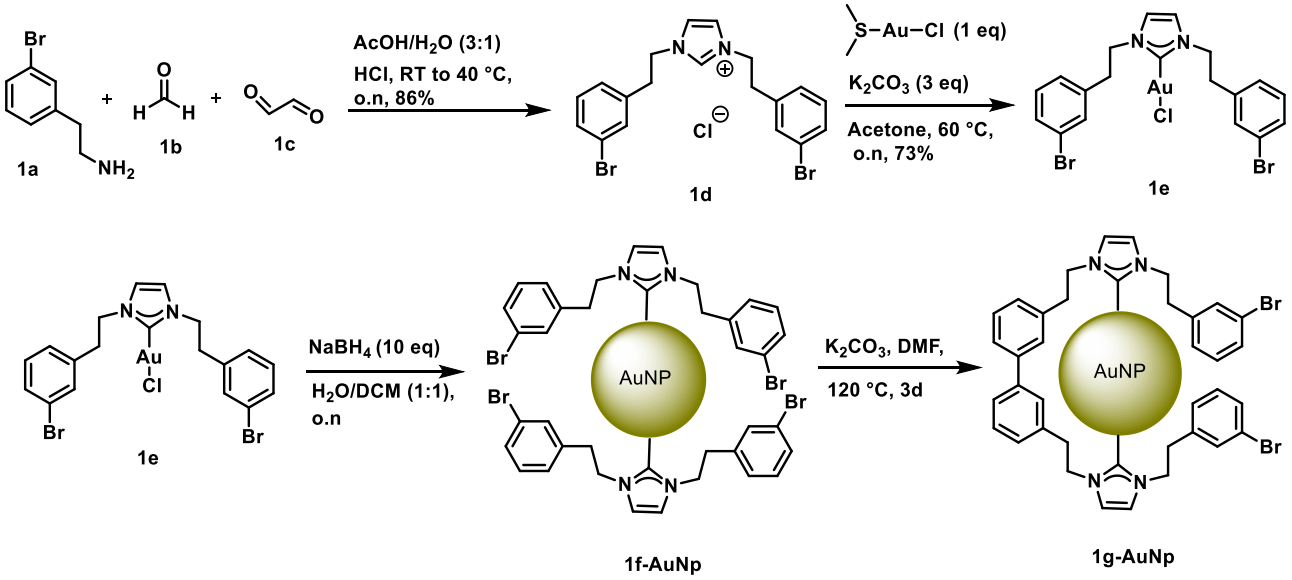

Scheme 2: Syntheses of NHC-functionalized AuNps, **1a** to **1g-AuNp**. For the functionalized Nps (**1f-AuNp** and **1g-AuNp)**, a condensed representation depicting two exemplary ligands are shown to illustrate the on-Np-surface reaction.

Results and Discussion

Synthesis and characterization of NHC-functionalized AuNps

We envisaged that the retrosynthesis of target compound **1f-AuNp**, could be obtained from a one-pot, three-component Mannich-type reaction of **1a**, **1b** and **1c** as opposed to imidazole alkylations or the use of orthoesters for symmetrical immidazolium salts, as reported in literature.[36–38] Therefore, we began with two equivalents of **1a** in AcOH/H_2O mixture (3:1) and introduced one equivalent of **1b** to form the corresponding diamine.[37] We then added one equivalent of **1c** to close the ring (Scheme 2). Addition of 3M HCl and heating the reaction to 40 °C furnished the imidazolium compound **1d** in 86% yield. ^{1}H-NMR of **1d** showed a diagnostic singlet at 10.26 ppm corresponding to the proton at the C2 position of the imidazolium ring, sandwiched by the two nitrogen atoms. Reaction of **1d** with K_2CO_3 furnished the *N*-heterocyclic carbene *in situ,* which was trapped with chloro(dimethylsulphide) gold (I) to give **1e** in 73% yield. The formation of **1e** was confirmed by loss of the singlet for the NHC proton appearing at 10.26 ppm in its ^{1}H-NMR spectrum, accompanied by an emergence of a signal at 183.22 ppm in the ^{13}C-NMR spectrum, corresponding to the carbene carbon atom of the C–Au bond. These two observations are indicative of successful *in situ* carbene generation and coordination to the gold(I) precursor.[39–41] Complex **1e** was reduced to the nanoparticles using a biphasic water/DCM medium as developed by Prezhdo, Brutchey, and co-workers for the synthesis of NHC-stabilized AgNps.[42,43] Unlike the monophasic media, biphasic solvent systems provide a different pathway with different reaction kinetics, in which the reduction of gold(I) complex takes place slowly, providing uniformly sized AuNps.[39,44] After aqueous workup, the resulting crude AuNps were thoroughly washed with tetrahydrofuran to remove any unbound ligand furnishing **1f-AuNp**.

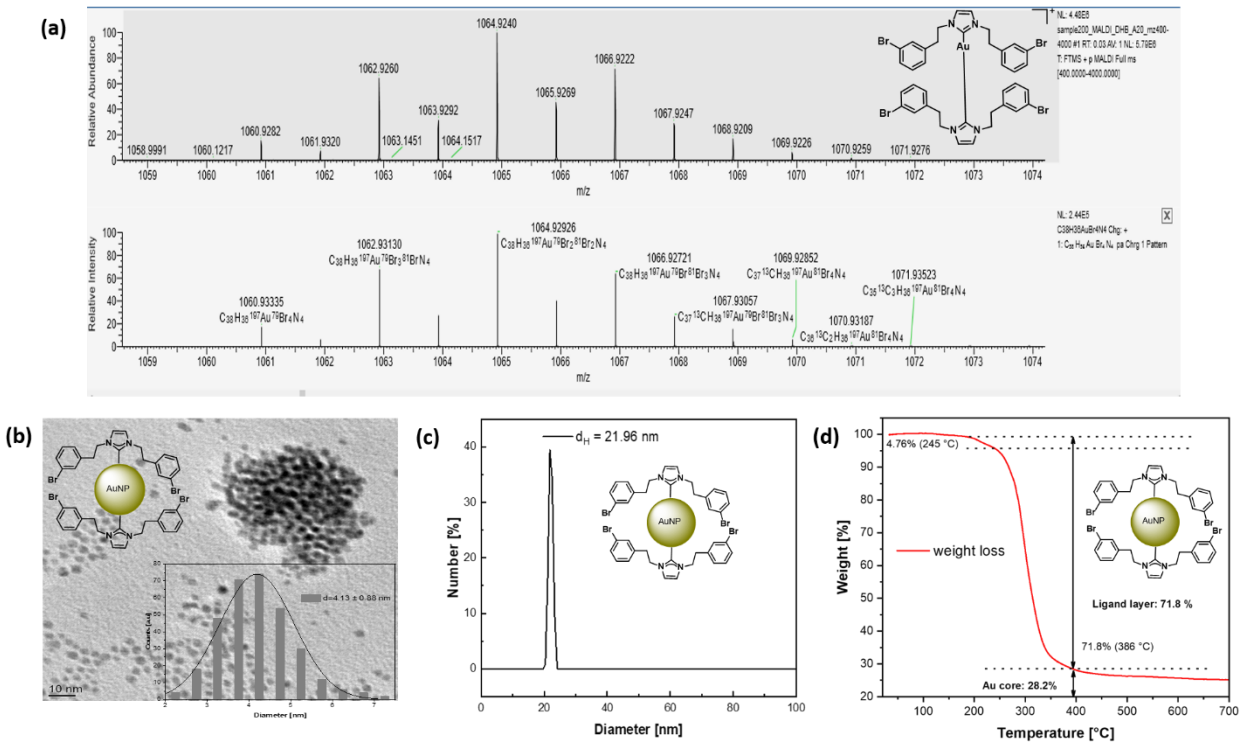

Figure 1: Characterization of **1f-AuNp**. (a) MALDI-MS spectra of **1f-AuNp**, bottom spectrum (simulated mass spectrum), and top (experimental mass spectrum). Spectra showed a mass peak at 1060.9282 (calc. 1060.9333), corresponding to $(NHC)_2Au^+$ fragmentation, indicating that the ligands are attached to the AuNps. (b) TEM and size distribution (inset) of **1f-AuNp** with an average diamenter of 4.10 ± 0.88 nm. (c) DLS spectrum of **1f-AuNp** with a hydrodynamic diameter of 22.0 nm and (d) Thermogram of **1f-AuNp**, with an NHC:Au core mass ratio of 72:28.

The functionalized AuNps were characterized with Matrix Assisted Laser Desorption Ionization Mass Spectrometry (MALDI-MS), Transmission Electron Microscopy (TEM), Dynamic Light Scattering (DLS), Thermogravimetric Analysis (TGA), Energy Dispersive X-ray Spectroscopy (EDX) and X-Ray Diffraction (XRD). Matrix-assisted and/or laser desorption/ionization mass spectrometry (MALDI-MS or LDI-MS) has proven to be a useful tool for the characterization of NHC's on AuNps and in some cases, shows the abstraction of gold adatoms, giving rise to $Au(NHC)_2$ species.[45–47] Similar results were obtained in the present study: a comparison of the simulated and the experimental MALDI-MS data can be explained by an abstraction of Au atom which gave rise to the mass peak at 1060.92 corresponding of $Au(NHC)_2$ motif (Figures 1a and S11). This result confirmed that we do not only have the AuNps but also have the ligands directly attached to the AuNps.

TEM analysis of the resulting Nps revealed the formation of spherical AuNps with an average diameter of 4.10 ± 0.88 nm (Figure 1b). However, this technique only enables the visualization of the nanoparticles' metallic core and excludes the organic shell of the Nps due to the much lower contrast of the organic shell, relative to the Au core.[40,41,48,49] We thereby employed dynamic light scattering (DLS) to measure the overall hydrodynamic diameter of the functionalized AuNps in dichloromethane (DCM). As shown in Figures 1c and S5**,** the hydrodynamic diameter of the dispersed AuNps in DCM, was estimated at ~22.0 nm. This increase in the hydrodynamic diameter is consistent with the fact that DLS measurements take into account the diameter of the gold core, NHC ligands attached to the AuNps, the electrostatic potential generated by the Nps as well as the entire solvent cage.

Thermogravimetric analysis (TGA) was used to determine the ratio of Au to NHC ligands in the resulting Nps (Figure 1d). There was a

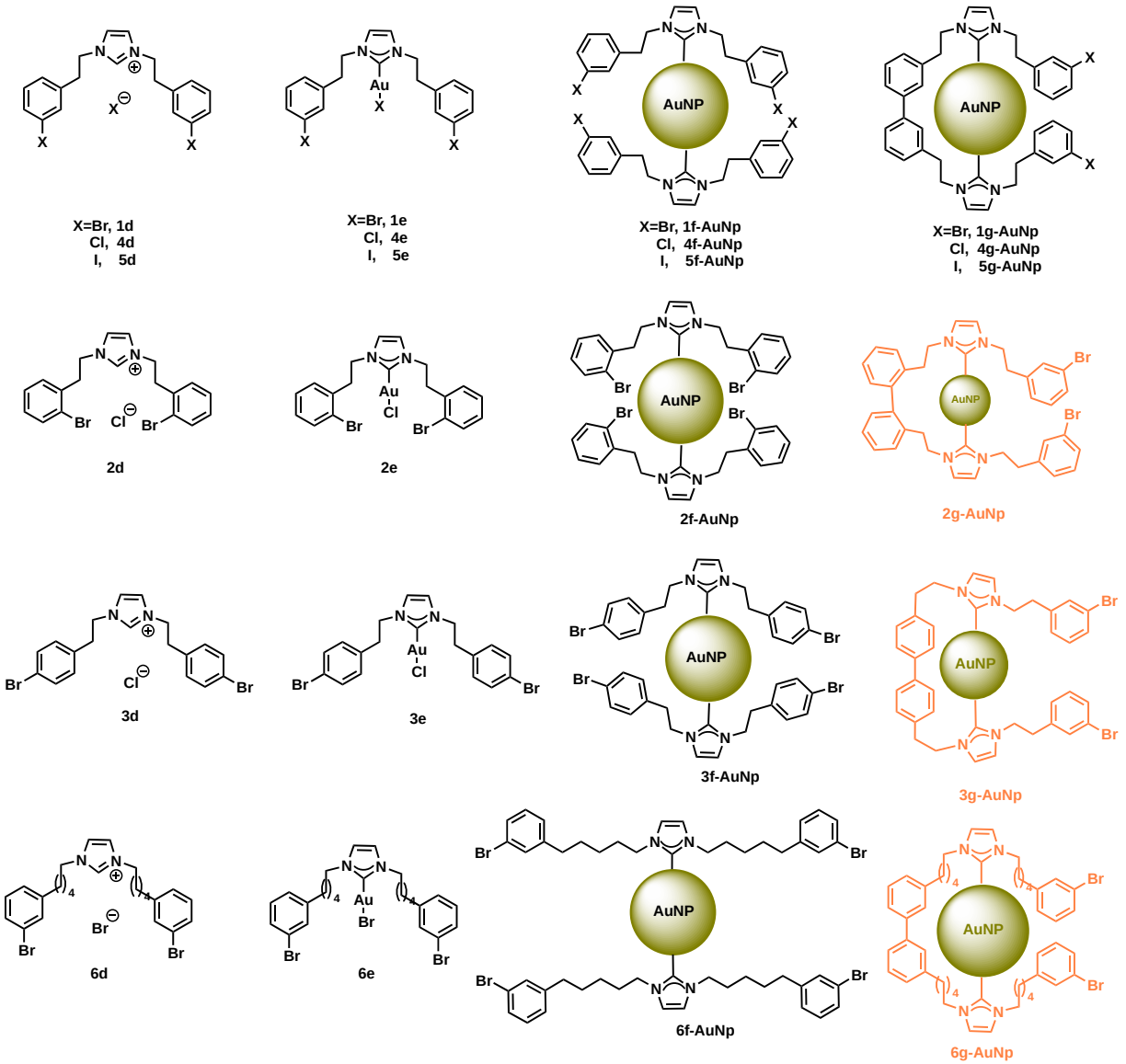

Figure 2: *N*-Heterocyclic carbenes studied in this work. The compounds marked on black were successfully synthesized, while those marked on red did not undergo on-surface Ullmann coupling reactions.

gradual decomposition at 245 °C, corresponding to 4.76 % weight loss of the functionalized Nps. At 248 to 382 °C, there was a massive decomposition corresponding to 71.8% of the entire mass of the Np. At higher temperatures up to 700 °C, no further phase change was observed indicating a 28.2% composition of the Au core. Taking into account, the weight percent of NHC from TGA analysis and the diameter of AuNps from TEM measurements, we were able to calculate the average number of NHCs on each Np following the method employed by Johnson and co-workers.[39] An average number of ≈2680 NHC molecules was present on the surface of the AuNp. Note that the NHC/**1f-AuNp** value might be inflated as it depends on the number of Au atoms in the Np, and the calculation of the number of Au atoms assumes a smooth spherical particle.[39] Nevertheless, this value indicates a high coverage of NHC per AuNp, as opposed to single molecules reported on a planar 2D Au surface.[22,23] In addition, the calculated value is in excellent agreement with literature reports for NHC-functionalized AuNps of similar core sizes.[28,39–41,44,48,50]

We employed energy dispersive X-ray spectroscopy (EDX) to determine the chemical composition of the AuNps. Peaks at 0.20, 0.24, 1.45 and 2.20 keV correspond to C Kα, N Kα, Br Lα, and Au Mα, respectively (Figure S7). Additionally, X-ray diffraction (XRD) profiles of the AuNps (Figure S9) showed reflexes at 38.5, 44.3, 64.5, and 77.7°, corresponding to Au (111), (200), (220), and (311) lattice

planes of Au, thus, indicating that the synthesized Nps is constructed from Au atoms.[51]

Ullmann coupling reaction on the surface of AuNps

As mentioned above, the design of the presented organic-inorganic hybrid system combines coupling partners, catalyst and reducing agent, all in one entity, with the aryl halides close to the surface of the Np.[27,32,52–54] Recent work by Camden and coworkers have shown that the geometry of these NHCs on nanoparticles is not far off from that on a 2D surface, and they rather exist in both flat and vertical configurations.[53] However, a linker molecule provides suitable distance between the aromatics and the AuNps. Several functional groups have been employed as linker molecules, but these functional groups have to be chemically inert towards the exact application of the hybrid material.[33–35,55,56] Moreover, a linker should be of optimum length, that minimizes electronic and steric effects between the AuNps and the aromatic moiety, while also enabling desired flexibility and motion of the entire ligand – that allows for onsurface reactivity – when attached to the AuNps. We thereby, settled for an ethylene chain as a linker, since it is chemically inert under Ullmann conditions, provides suitable distance between the AuNps and the aromatic moiety, and in turn, avoids the flipping away of the reacting partner, which arises from a high degree of flexibility of ligands with long chain lengths, when attached to the Nps.[56,57]

With these criteria in mind, we selected **1f-AuNp**, which has a linker of two carbon atoms, with the bromine situated at the *meta*-position (Figure 2). Accordingly, reaction of **1f-AuNp** with 12 equivalents of K_2CO_3 furnished **1g-AuNp**. We employed attenuated total reflectance infrared spectroscopy (ATR-IR) and surface enhanced raman spectroscopy (SERS) to analyze the successful coupling reaction on the surface of AuNps, which were used in characterizing similar hybrid systems.[32,39,41,48,53,54,58,59] IR spectra showed a strong reduction in the intensity of the band at 1070 cm^{-1}, which is assigned to the C–Br vibration frequency. This decrease indicates that some of the C–Br bonds have been replaced by another, a C–C bond (Figure 3a). The rest of the spectrum was unperturbed, indicating that the functionalized AuNp was only modified at the bromine position. In addition, SERS spectra showed a complete disappearance of the band at 665 cm^{-1}(C–Br bond), relative to the SERS spectrum before the reaction.

EDX analysis of the reacted Np showed a 10.5% increase in the C composition of the sample, 11.7% decrease in Br composition, and a corresponding 0.3% decrease in Au composition (Figures S7 to S8). These observations are also in accordance with a coupling reaction at the C–Br since Ullmann reaction is driven by the leaching of Au to AuBr. The loss of Au in Ullmann reaction has been observed and reported in literature. For example, the group of Kantam observed 9.5 % leaching of Au with a significant decrease in yield after three cycles of Ullmann reaction.[60] Similarly, the group of Jin also observed leaching of Au in Ullmann reaction, with a resulting decrease in reaction yield after about five cycles.[61] Moreover, the observation that bromine can still be traced in the composition of **1g-AuNp** suggests that the reaction did not reach 100% conversion. It contained both the reacted and the unreacted ligands, attached to the same surface of the AuNp. However, the formation of Aryl-Au bonds via oxidative addition is rather unlikely, as several reports have shown that in Au-promoted Ullmann reactions, the process does not stop at the stage of oxidative addition. In this case, the cycle of reductive elimination is completed and eventually the C–C coupling product is formed.[61–65]

Furthermore, the on-Np-surface coupling reaction was confirmed with MALDI-MS. MALDI-MS spectra showed a mass peak at 903.09 corresponding to the mass of **1g-AuNp** with an abstraction of Au atom in the form of $Au(NHC)_2$ motif, just as expected (Figure S13). Thus, indicating that the successful on-surface reaction of the aryl moiety of **1f-AuNp** was achieved. This spectrum was also in perfect agreement with the calculated spectrum for the proposed structure on the surface of the AuNp (Figure S13). In addition, we observed a MALDI mass peak of two coupled units with two open ring dimers, which is in correspondence with the reduction of C–Br band observed in the SERS and IR spectra (Figure S14). This result supports that the on-Np-surface reaction is not limited to two coupling units but can exist in a chain-like manner, leading to multiple coupled units on the surface of the AuNps. Nonetheless, MALDI analyses of **1g-AuNp** also showed the mass of the starting material at 432.99 (Figure S12) corresponding to the mass observed in the ESI-MS of **Id** (page S4). These data also corroborate the results of EDX spectroscopy, which allude that the reacted nanoparticles comprise of both the reacted and unreacted NHC-ligands bound to the same surface of the AuNp.

Next, we attempted an intermolecular hetero Ullmann coupling of compound **1f-AuNp** with *p*-bromobenzonitrile under the same reaction conditions for the intramolecular homo Ullmann reaction. However, there was no evidence for a hetero coupling reaction between **1f-AuNp** and *p*-bromobenzonitrile, suggesting that the tilted geometry of the carbenes leads preferable to an intramolecular homo over intermolecular hetero Ullmann reaction.

We then probed how the proximity of the halogen towards the surface of AuNps influences on-Np-surface Ullmann reaction, by varying the Br substitution from *meta* to *ortho* and *para* positions, and repeated the Ullmann reactions with the above conditions applied for **1f-AuNp**. However, we were unable to obtain the expected products (**2g-AuNp** and **3g-AuNp)**. SERS of **3g-AuNp** and ATR-IR spectroscopy of **2g-AuNp** showed a reasonable retention of the starting material, with SERS bands at 631, 770 and 1071 cm^{-1} (Figure S21), corresponding to C–Br bond, C–C aliphatic chain at the wingtip position, and benzene groups, respectively. This result can be rationalized as the two Br atoms from two adjacent aryl units need to be in proximity with the Au surface to enable an oxidative addition followed by a reductive elimination, which then furnishes the

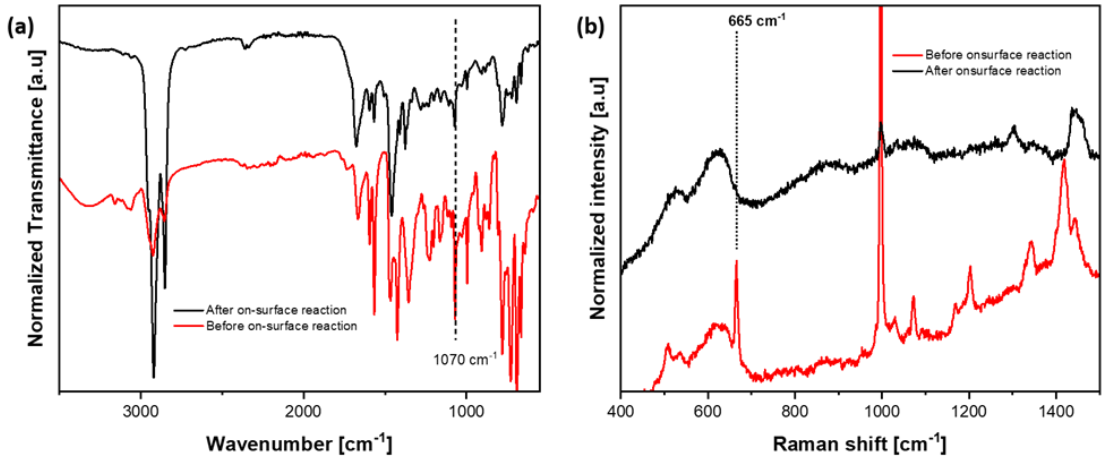

Figure 3: Ullmann coupling of **1f-AuNp**. (a) IR spectra and (b) SERS spectra AuNps before reaction (red) and after Ullmann reaction (black).

coupled product on the Np. In the case of **2f-AuNp** and **3f-AuNp**, the geometry does not fit and no insertion can occur.

Additionally, we tested the reactivity of different halogens towards on-Np-surface coupling reactions by varying the halogen from Br to Cl and I. Applying the same reaction conditions, we were unable to obtain the desired coupling product, **4g-AuNp** and **5g-AuNp**. SERS spectrum of **5g-AuNp** deviated from that of the starting material, **5f-AuNp** (Figure S22). There was a remarked intensification of C-C aliphatic chains due to the pronounced band at 733 cm^{-1}. In addition, there was a slight retention of aromatic rings due to the band at 998 cm^{-1}. These two concurrent observations indicate a degradation of **5f-AuNp** at the temperature of reaction. In addition, ATR-IR spectrum of **5g-AuNp** showed significant broadening of the signals and appearance of new bands relative to the starting material (Figure S18), bolstering the conclusion from the SERS data. This is plausible, as aryl iodides have been reported to be more reactive than its bromide and chloride counterparts, requiring lower temperatures of activation in the in-solution as well as the on-surface coupling reactions.[66] To also validate this known phenomenon for on-Np-surface reactivity, we repeated the on-surface Ullmann reaction of **5f-AuNp** while reducing the reaction temperature from 120 to 100 °C. Under these conditions, we were able to obtain **5g-AuNp**, whose coupling product is essentially the same as that made from the previously studied precursor, **1f-AuNp** (Figure S20).

Also, for **4f-AuNp,** no coupling was observed. This is expected and in accordance to the lower reactivity of Aryl chlorides. Interestingly, TEM analysis of **4f-AuNp** showed deviation to the other Nps, such as lack of size uniformities, slight distortion in core shapes and increased diameters of these Nps with an average Au core size of 34.5 $\pm$ 24.4 nm (Figure S3). Therefore, this behavior could not be excluded to explain the unsuccessful formation of **4g-AuNp**, since surface reaction and surface catalysis are dependent on shapes, sizes, porosity, diffusion rate and surface areas of Nps.[67]

Next, we studied how the orientation of the entire reaction partner towards the AuNp influences reactivity on the Np-surfaces. We varied the length of the linker from C_2 to C_5 and repeated the same Ullmann reaction. Again, we were unable to obtain the coupling product **6g-AuNp** from **6f-AuNp**. This can be attributed to the fact that, the coupling partners are too flexible and can flip away from the surface of the Np to minimize sterics, which in turn, minimizes the proximity between the aryl halide moiety and the surface of the AuNp. In addition, it has been established, that NHC ligands can move easily on surfaces via a unique ballbot-type motion, in which the NHC first pulls out an Au adatom (as also observed in this study), and then rides on it across the surface.[23,32,54,68] This distinctive mode of mobility is fundamental to the formation of surface assembled monolayers (SAMs). This ballbot-type motion is more and more hindered as the ligand size increases and is therefore, a function of the ligand size and ligand electronics.[23,68] Thus, a combination of the aforementioned effects can rationalize the lack of reactivity of **6f-AuNp** towards Ullmann reaction.

We proceeded with further characterization of the successfully functionalized AuNp (that is **1g-AuNp**), to determine the nature and/or existence of the nanoparticles after on-Np-surface Ullmann reaction. TEM showed an increase in core sizes with an average core size of 16.8 ± 8.92 nm (Figure S4). Additionally, DLS spectrum of **1g-AuNp** (Figure S6), revealed a hydrodynamic diameter of 33.8 nm with a zeta potential value of 0.180 mV, which is suggestive of a neutrally charged ligand and a tendency of precipitation when dispersed in CH_2Cl_2. EDX analyses of **1g-AuNp** showed Au Mα signal at 2.2 keV, suggesting the retention of the AuNps after reaction. In addition, XRD profile of the reacted AuNps showed reflexes at at 38.5, 44.3, 64.5, and 77.7°, which correlate to the face-centered

cubic unit cell of AuNps. It is noteworthy to mention that the XRD reflexes became more pronounced relative to the AuNp prior to the on-surface reaction. This phenomenon is due to increase in sizes, as the reflexes due to AuNps become relatively more pronounced in this size regime.[51] This observation is in accordance with the result of the TEM and DLS measurements. The abstraction of Au adatom by the reacted ligands - which was observed by MALDI MS experiments - also suggest the retention of these Nps after being subjected to Ullmann reaction conditions. All data point to the fact that the nanoparticles still remained as nanoparticles after having undergone a successful on-surface Ullmann reaction.

Conclusion

By varying the planar 2D surfaces of gold(111) to a rough surface of gold nanoparticles and fine-tuning the different segments of a hybrid material, we were able to utilize the bonding geometry of NHCs on AuNps to successfully achieve an Ullmann coupling of aryl halide moieties connected via NHC on a one-system hybrid material functioning as the catalyst and reacting partner. The synthesis of the nanoparticles was characterized by combination of MALDI-MS, TEM, DLS, TGA, zeta potential values, EDX, and, XRD. While reactions and retention of the nanoparticles were confirmed by combination of IR, SERS, EDX, MALDI-MS, XRD, TEM, DLS, We studied how the nature of the halogens, proximity of the halogen and that of the reacting partner on the surface of the Nps, influences the reactivity on surfaces. Our work proves that an appropriate organic ligand, suitable halogen position, moderate chain length, and moderate reactivity of halogen are influential towards selectivities of Ullmann coupling on AuNps, thus, opening new prospects in organic on-surface synthesis to a promising class of organic-metal hybrid materials.

Data availability

General information, synthetic procedure, TEM, DLS, EDX analysis, XRD, MALDI spectra, ATR-IR, SERS, NMR spectra, and additional references are provided in the Supporting document.

Author Contributions

H.A. Wegner conceptualized the project and interpreted the data. N. Ukah modified the concept, implemented it, conducted all experiments, interpreted the data and analyzed all results. Both authors were involved in the manuscript preparation.

Conflicts of interest

There are no conflicts to declare.

Acknowledgements

This work was supported by the LOEWE Program of Excellence of the Federal State of Hesse (LOEWE Focus Group PriOSS 'Principles of On-Surface Synthesis') and Justus Liebig University, Giessen, Germany. In addition, the authors wish to express their sincere gratitude to Anne Schulze, Limei Chen, Max Müller, Klaus Peppler and Christian Bauer for the TEM, SERS, MALDI, EDX and XRD measurements.

References

1 A. V. Zhukhovitskiy, M. J. MacLeod and J. A. Johnson, Carbene Ligands in Surface Chemistry: From Stabilization of Discrete Elemental Allotropes to Modification of Nanoscale and Bulk Substrates, *Chem. Rev.*, 2015, **115**, 11503–11532.

2 C.-Y. Wu, W. J. Wolf, Y. Levartovsky, H. A. Bechtel, M. C. Martin, F. D. Toste and E. Gross, High-spatial-resolution mapping of catalytic reactions on single particles, *Nature*, 2017, **541**, 511–515.

3 C. A. Smith, M. R. Narouz, P. A. Lummis, I. Singh, A. Nazemi, C.-H. Li and C. M. Crudden, N-Heterocyclic Carbenes in Materials Chemistry, *Chem. Rev.*, 2019, **119**, 4986–5056.

4 K. A. Simonov, N. A. Vinogradov, A. S. Vinogradov, A. V. Generalov, E. M. Zagrebina, G. I. Svirskiy, A. A. Cafolla, T. Carpy, J. P. Cunniffe, T. Taketsugu, A. Lyalin, N. Mårtensson and A. B. Preobrajenski, From Graphene Nanoribbons on Cu(111) to Nanographene on Cu(110): Critical Role of Substrate Structure in the Bottom-Up Fabrication Strategy, *ACS nano*, 2015, **9**, 8997–9011.

5 Q. Shen, H.-Y. Gao and H. Fuchs, Frontiers of on-surface synthesis: From principles to applications, *Nano Today*, 2017, **13**, 77–96.

6 P. Ruffieux, S. Wang, B. Yang, C. Sánchez-Sánchez, J. Liu, T. Dienel, L. Talirz, P. Shinde, C. A. Pignedoli, D. Passerone, T. Dumslaff, X. Feng, K. Müllen and R. Fasel, On-surface synthesis of graphene nanoribbons with zigzag edge topology, *Nature*, 2016, **531**, 489–492.

7 R. Pawlak, X. Liu, S. Ninova, P. D'Astolfo, C. Drechsel, S. Sangtarash, R. Häner, S. Decurtins, H. Sadeghi, C. J. Lambert, U. Aschauer, S.-X. Liu and E. Meyer, Bottom-up Synthesis of Nitrogen-Doped Porous Graphene Nanoribbons, *J. Am. Chem Soc.*, 2020, **142**, 12568–12573.

8 J. C. Love, L. A. Estroff, J. K. Kriebel, R. G. Nuzzo and G. M. Whitesides, Self-assembled monolayers of thiolates on metals as a form of nanotechnology, *Chem. Rev.*, 2005, **105**, 1103–1169.

9 M. Koy, P. Bellotti, M. Das and F. Glorius, N-Heterocyclic carbenes as tunable ligands for catalytic metal surfaces, *Nat. Catal*, 2021, **4**, 352–363.

10 C. J. Judd, F. L. Q. Junqueira, S. L. Haddow, N. R. Champness, D. A. Duncan, R. G. Jones and A. Saywell, Structural characterisation of molecular conformation and the incorporation of adatoms in an on-surface Ullmann-type reaction, *Commun. Chem*, 2020, **3**, 166.

11 L. Grossmann, D. A. Duncan, S. P. Jarvis, R. G. Jones, S. De, J. Rosen, M. Schmittel, W. M. Heckl, J. Björk and M. Lackinger, Evolution of adsorption heights in the on-surface synthesis and decoupling of covalent organic networks on Ag(111) by normal-incidence X-ray standing wave, *Nanoscale Horiz*, 2021, **7**, 51–62.

12 L. Grill and S. Hecht, Covalent on-surface polymerization, *Nat. Chem*, 2020, **12**, 115–130.

13 M. Fritton, D. A. Duncan, P. S. Deimel, A. Rastgoo-Lahrood, F. Allegretti, J. V. Barth, W. M. Heckl, J. Björk and M. Lackinger, The Role of Kinetics versus Thermodynamics in Surface-Assisted Ullmann Coupling on Gold and Silver Surfaces, *J. Am. Chem Soc.*, 2019, **141**, 4824–4832.

14 J. Eichhorn, D. Nieckarz, O. Ochs, D. Samanta, M. Schmittel, P. J. Szabelski and M. Lackinger, On-surface Ullmann coupling: the influence of kinetic reaction parameters on the morphology and quality of covalent networks, *ACS nano*, 2014, **8**, 7880–7889.

15 M. Di Giovannantonio, M. Tomellini, J. Lipton-Duffin, G. Galeotti, M. Ebrahimi, A. Cossaro, A. Verdini, N. Kharche, V. Meunier, G. Vasseur, Y. Fagot-Revurat, D. F. Perepichka, F. Rosei and G. Contini, Mechanistic Picture and Kinetic Analysis of Surface-Confined Ullmann Polymerization, *J. Am. Chem Soc.*, 2016, **138**, 16696–16702.

16 M. Di Giovannantonio, M. El Garah, J. Lipton-Duffin, V. Meunier, L. Cardenas, Y. Fagot Revurat, A. Cossaro, A. Verdini, D. F. Perepichka, F. Rosei and G. Contini, Insight into organometallic intermediate and its evolution to covalent bonding in surface-confined ullmann polymerization, *ACS nano*, 2013, **7**, 8190–8198.

17 C. M. Crudden, J. H. Horton, M. R. Narouz, Z. Li, C. A. Smith, K. Munro, C. J. Baddeley, C. R. Larrea, B. Drevniok, B. Thanabalasingam, A. B. McLean, O. V. Zenkina, I. I. Ebralidze, Z. She, H.-B. Kraatz, N. J. Mosey, L. N. Saunders and A. Yagi, Simple direct formation of self-assembled N-heterocyclic carbene monolayers on gold and their application in biosensing, *Nat. Commun.*, 2016, **7**, 12654.

18 C. M. Crudden, J. H. Horton, I. I. Ebralidze, O. V. Zenkina, A. B. McLean, B. Drevniok, Z. She, H.-B. Kraatz, N. J. Mosey, T. Seki, E. C. Keske, J. D. Leake, A. Rousina-Webb and G. Wu, Ultra stable self-assembled monolayers of N-heterocyclic carbenes on gold, *Nat. Chem*, 2014, **6**, 409–414.

19 S. Clair and D. G. de Oteyza, Controlling a Chemical Coupling Reaction on a Surface: Tools and Strategies for On-Surface Synthesis, *Chem. Rev.*, 2019, **119**, 4717–4776.

20 P. Bellotti, M. Koy, M. N. Hopkinson and F. Glorius, Recent advances in the chemistry and applications of N-heterocyclic carbenes, *Nat. Rev. Chem.*, 2021, **5**, 711–725.

21 S. Amirjalayer, A. Bakker, M. Freitag, F. Glorius and H. Fuchs, Cooperation of N-Heterocyclic Carbenes on a Gold Surface, *Angew. Chem., Int. Ed.*, 2020, **59**, 21230–21235.

22 Q. Zhong, A. Ihle, S. Ahles, H. A. Wegner, A. Schirmeisen and D. Ebeling, Constructing covalent organic nanoarchitectures molecule by molecule via scanning probe manipulation, *Nat. Chem*, 2021, **13**, 1133–1139.

23 J. Ren, M. Koy, H. Osthues, B. S. Lammers, C. Gutheil, M. Nyenhuis, Q. Zheng, Y. Xiao, L. Huang, A. Nalop, Q. Dai, H.-J. Gao, H. Mönig, N. L. Doltsinis, H. Fuchs and F. Glorius, On-surface synthesis of ballbot-type N-heterocyclic carbene polymers, *Nat. Chem*, 2023, **15**, 1737–1744.

24 T. Shirman, R. Kaminker, D. Freeman and M. E. van der Boom, Halogen-bonding mediated stepwise assembly of gold nanoparticles onto planar surfaces, *ACS nano*, 2011, **5**, 6553–6563.

25 K. Buntara Sanjeeva, C. Pigliacelli, L. Gazzera, V. Dichiarante, F. Baldelli Bombelli and P. Metrangolo, Halogen bond-assisted self-assembly of gold nanoparticles in solution and on a planar surface, *Nanoscale*, 2019, **11**, 18407–18415.

26 S.-H. Kim, E.-M. Kim, C.-M. Lee, D. W. Kim, S. T. Lim, M.-H. Sohn and H.-J. Jeong, Synthesis of PEG-Iodine-Capped Gold Nanoparticles and Their Contrast Enhancement in In Vitro and In Vivo for X-Ray/CT, *J. Nanomater.*, 2012, **2012**.

27 Y. Kim, S. Ji and J.-M. Nam, A Chemist's View on Electronic and Steric Effects of Surface Ligands on Plasmonic Metal Nanostructures, *Acc. Chem. Res*, 2023, **56**, 2139–2150.

28 M. W. Brett, C. K. Gordon, J. Hardy and N. J. L. K. Davis, The Rise and Future of Discrete Organic-Inorganic Hybrid Nanomaterials, *ACS Phys. Chem. Au.*, 2022, **2**, 364–387.

29 D. A. Hines and P. V. Kamat, Recent advances in quantum dot surface chemistry, *ACS Appl Mater Interfaces*, 2014, **6**, 3041–3057.

30 L. M. Rossi, J. L. Fiorio, M. A. S. Garcia and C. P. Ferraz, The role and fate of capping ligands in colloidally prepared metal nanoparticle catalysts, *Dalton Trans.*, 2018, **47**, 5889–5915.

31 J. de Roo, M. Ibáñez, P. Geiregat, G. Nedelcu, W. Walravens, J. Maes, J. C. Martins, I. van Driessche, M. V. Kovalenko and Z. Hens, Highly Dynamic Ligand Binding and Light Absorption Coefficient of Cesium Lead Bromide Perovskite Nanocrystals, *ACS nano*, 2016, **10**, 2071–2081.

32 S. Dery, W. Cao, C. Yao and C. Copéret, NMR Spectroscopic Signatures of Cationic Surface Sites from Supported Coinage Metals Interacting with N-Heterocyclic Carbenes, *J. Am. Chem Soc.*, 2024.

33 Z. Huang and M. L. Tang, Designing Transmitter Ligands That Mediate Energy Transfer between Semiconductor Nanocrystals and Molecules, *J. Am. Chem Soc.*, 2017, **139**, 9412–9418.

34 Z. Huang, Z. Xu, T. Huang, V. Gray, K. Moth-Poulsen, T. Lian and M. L. Tang, Evolution from Tunneling to Hopping Mediated Triplet Energy Transfer from Quantum Dots to Molecules, *J. Am. Chem Soc.*, 2020, **142**, 17581–17588.

35 X. Li, Z. Huang, R. Zavala and M. L. Tang, Distance-Dependent Triplet Energy Transfer between CdSe Nanocrystals and Surface Bound Anthracene, *J. Phys. Chem. Lett.*, 2016, **7**, 1955–1959.

36 L. Benhamou, E. Chardon, G. Lavigne, S. Bellemin-Laponnaz and V. César, Synthetic routes to N-heterocyclic carbene precursors, *Chem. Rev.*, 2011, **111**, 2705–2733.

37 M. H. Dunn, N. Konstandaras, M. L. Cole and J. B. Harper, Targeted and Systematic Approach to the Study of pKa Values of Imidazolium Salts in Dimethyl Sulfoxide, *J. Org. Chem.*, 2017, **82**, 7324–7331.

38 K. M. Kuhn and R. H. Grubbs, A facile preparation of imidazolinium chlorides, *Org. Lett.*, 2008, **10**, 2075–2077.

39 M. J. MacLeod and J. A. Johnson, PEGylated N-Heterocyclic Carbene Anchors Designed To Stabilize Gold Nanoparticles in Biologically Relevant Media, *J. Am. Chem Soc.*, 2015, **137**, 7974–7977.

40 N. A. Nosratabad, Z. Jin, L. Du, M. Thakur and H. Mattoussi, N-Heterocyclic Carbene-Stabilized Gold Nanoparticles: Mono- Versus Multidentate Ligands, *Chem. Mater.*, 2021, **33**, 921–933.

41 M. Bélanger-Bouliga, R. Mahious, P. I. Pitroipa and A. Nazemi, Perylene diimide-tagged N-heterocyclic carbene-stabilized gold nanoparticles: How much ligand desorbs from surface in presence of thiols?, *Dalton Trans.*, 2021, **50**, 5598–5606.

42 H. Lu and R. L. Brutchey, Tunable Room-Temperature Synthesis of Coinage Metal Chalcogenide Nanocrystals from N -Heterocyclic Carbene Synthons, *Chem. Mater.*, 2017, **29**, 1396–1403.

43 H. Lu, Z. Zhou, O. V. Prezhdo and R. L. Brutchey, Exposing the Dynamics and Energetics of the N-Heterocyclic Carbene-Nanocrystal Interface, *J. Am. Chem Soc.*, 2016, **138**, 14844–14847.

44 M. R. Narouz, C.-H. Li, A. Nazemi and C. M. Crudden, Amphiphilic N-Heterocyclic Carbene-Stabilized Gold Nanoparticles and Their Self-Assembly in Polar Solvents, *Langmuir.*, 2017, **33**, 14211–14219.

45 N. L. Dominique, I. M. Jensen, G. Kaur, C. Q. Kotseos, W. C. Boggess, D. M. Jenkins and J. P. Camden, Giving Gold Wings: Ultrabright and Fragmentation Free Mass Spectrometry Reporters for Barcoding, Bioconjugation Monitoring, and Data Storage, *Angew. Chem., Int. Ed.*, 2023, **62**, e202219182.

46 N. L. Dominique, S. L. Strausser, J. E. Olson, W. C. Boggess, D. M. Jenkins and J. P. Camden, Probing N-Heterocyclic Carbene Surfaces with Laser Desorption Ionization Mass Spectrometry, *Anal. Chem.*, 2021, **93**, 13534–13538.

47 G. Kaur, N. L. Dominique, G. Hu, P. Nalaoh, R. L. Thimes, S. L. Strausser, L. Jensen, J. P. Camden and D. M. Jenkins, Reactivity variance between stereoisomers of saturated N-heterocyclic carbenes on gold surfaces, *Inorg. Chem. Front.*, 2023, **10**, 6282–6293.

48 J. F. DeJesus, L. M. Sherman, D. J. Yohannan, J. C. Becca, S. L. Strausser, L. F. P. Karger, L. Jensen, D. M. Jenkins and J. P. Camden, A Benchtop Method for Appending Protic Functional Groups to N-Heterocyclic Carbene Protected Gold Nanoparticles, *Angew. Chem., Int. Ed.*, 2020, **132**, 7655–7660.

49 E. L. Albright, T. I. Levchenko, V. K. Kulkarni, A. I. Sullivan, J. F. DeJesus, S. Malola, S. Takano, M. Nambo, K. Stamplecoskie, H. Häkkinen, T. Tsukuda and C. M. Crudden, N-Heterocyclic Carbene-Stabilized Atomically Precise Metal Nanoclusters, *J. Am. Chem Soc.*, 2024, **146**, 5759–5780.

50 T. C. Jones, L. Sumner, G. Ramakrishna, M. b. Hatshan, A. Abuhagr, S. Chakraborty and A. Dass, Bulky t -Butyl Thiolated Gold Nanomolecular Series: Synthesis, Characterization, Optical Properties, and Electrocatalysis, *J. Phys. Chem.*, 2018, **122**, 17726–17737.

51 S. Krishnamurthy, A. Esterle, N. C. Sharma and S. V. Sahi, Yucca-derived synthesis of gold nanomaterial and their catalytic potential, *Nanoscale Res. Lett.*, 2014, **9**, 627.

52 G. Kaur, R. L. Thimes, J. P. Camden and D. M. Jenkins, Fundamentals and applications of N-heterocyclic carbene functionalized gold surfaces and nanoparticles, *Chem. Comm.*, 2022, **58**, 13188–13197.

53 R. L. Thimes, A. V. B. Santos, R. Chen, G. Kaur, L. Jensen, D. M. Jenkins and J. P. Camden, Using Surface-Enhanced Raman Spectroscopy to Unravel the Wingtip-Dependent Orientation of N-Heterocyclic Carbenes on Gold Nanoparticles, *J. Phys. Chem. Lett.*, 2023, **14**, 4219–4224.

54 J. M. Palasz, Z. Long, J. Meng, P. E. Videla, H. R. Kelly, T. Lian, V. S. Batista and C. P. Kubiak, A Resilient Platform for the Discrete Functionalization of Gold Surfaces Based on N-Heterocyclic Carbene Self-Assembled Monolayers, *J. Am. Chem Soc.*, 2024.

55 V. Gray, Z. Zhang, S. Dowland, J. R. Allardice, A. M. Alvertis, J. Xiao, N. C. Greenham, J. E. Anthony and A. Rao, Thiol-Anchored TIPS-Tetracene Ligands with Quantitative Triplet Energy Transfer to PbS Quantum Dots and Improved Thermal Stability, *J. Phys. Chem. Lett.*, 2020, **11**, 7239–7244.

56 C. Xia, W. Wang, L. Du, F. T. Rabouw, D. van den J. Heuvel, H. C. Gerritsen, H. Mattoussi and C. de Mello Donega, Förster Resonance Energy Transfer between Colloidal CuInS 2 /ZnS Quantum Dots and Dark Quenchers, *J. Phys. Chem.*, 2020, **124**, 1717–1731.

57 A. Rossi, M. B. Price, J. Hardy, J. Gorman, T. W. Schmidt and N. J. L. K. Davis, Energy Transfer between Perylene Diimide Based Ligands and Cesium Lead Bromide Perovskite Nanocrystals, *J. Phys. Chem.*, 2020, **124**, 3306–3313.

58 L. M. Sherman, M. D. Finley, R. K. Borsari, N. Schuster-Little, S. L. Strausser, R. J. Whelan, D. M. Jenkins and J. P. Camden, N-Heterocyclic Carbene Ligand Stability on Gold Nanoparticles in Biological Media, *ACS omega*, 2022, **7**, 1444–1451.

59 M. J. Trujillo, S. L. Strausser, J. C. Becca, J. F. DeJesus, L. Jensen, D. M. Jenkins and J. P. Camden, Using SERS To Understand the Binding of N-Heterocyclic Carbenes to Gold Surfaces, *J. Phys. Chem. Lett.*, 2018, **9**, 6779–6785.

60 K. Layek, H. Maheswaran and M. L. Kantam, Ullmann coupling of aryl iodides catalyzed by gold nanoparticles stabilized on nanocrystalline magnesium oxide, *Catal. Sci. Technol.,*, 2013, **3**, 1147.

61 G. Li, C. Liu, Y. Lei and R. Jin, Au25 nanocluster-catalyzed Ullmann-type homocoupling reaction of aryl iodides, *Chem Comm*, 2012, **48**, 12005–12007.

62 B. Karimi and F. K. Esfahani, Unexpected golden Ullmann reaction catalyzed by Au nanoparticles supported on periodic mesoporous organosilica (PMO), *Chem Comm*, 2011, **47**, 10452–10454.

63 K. Layek, H. Maheswaran and M. L. Kantam, Ullmann coupling of aryl iodides catalyzed by gold nanoparticles stabilized on nanocrystalline magnesium oxide, *Catal. Sci. Technol.,*, 2013, **3**, 1147.

64 G. Li and R. Jin, Catalysis by gold nanoparticles: carbon-carbon coupling reactions, *Nano Rev.*, 2013, **2**, 529–545.

65 A. Monopoli, P. Cotugno, G. Palazzo, N. Ditaranto, B. Mariano, N. Cioffi, F. Ciminale and A. Nacci, Ullmann Homocoupling Catalysed by Gold Nanoparticles in Water and Ionic Liquid, *ASC*, 2012, **354**, 2777–2788.

66 F. Khan, M. Dlugosch, X. Liu and M. G. Banwell, The Palladium-Catalyzed Ullmann Cross-Coupling Reaction: A Modern Variant on a Time-Honored Process, *Acc. Chem. Res*, 2018, **51**, 1784–1795.

67 W. Grunert, W. Kleist and M. Muhler, *Catalysis at surfaces*, De Gruyter, Berlin, Boston, 2023.

68 G. Wang, A. Rühling, S. Amirjalayer, M. Knor, J. B. Ernst, C. Richter, H.-J. Gao, A. Timmer, H.-Y. Gao, N. L. Doltsinis, F. Glorius and H. Fuchs, Ballbot-type motion of N-heterocyclic carbenes on gold surfaces, *Nat. Chem.*, 2017, **9**, 152–156.

Abbreviation

AFM	Atomic Force Microscopy
AuNps	Gold Nanoparticles
CTAB	Cetyl trimethylammonium Bromide
d	Day
DCM	Dichloromethane
DFT	Density Functional Theory
DLS	Dynamic Light Scattering
EDX	Energy Dispersive X-ray Spectroscopy
HOMO	Highest Occupied Molecular Orbital
HREELS	High Electron Energy Loss Spectroscopy
HSAB	Hard Soft Lewis Acids and Bases
FTIR	Fourier Transform Infrared Spectroscopy
LSPR	Localized Surface Plasmon Resonance
LUMO	Lowest Unoccupied Molecular Orbital
m	*meta*
MALDI-TOF	Matrix Assisted Laser Desorption Ionization Time Of Flight
min	Minute
mol	Mole
NEXAFS	Near Edge X-ray Absorption Fine Structure Spectroscopy
NHC	*N*-Heterocyclic Carbene
NIR	Near Infrared
nm	Nanometer
NMR	Nuclear Magnetic Resonance
o	*ortho*
p	*para*
PDOS	Projected Density of States
RPM	Rounds Per Minute

SAM	Surface Assembled Monolayer
SERS	Surface Enhanced Raman Scattering
SIMS	Secondary Ion Mass Spectroscopy
SPR	Surface Plasmon Resonance
STM	Scanning Tunnelling Microscope
TEM	Transmission Electron Microscope
TOAB	Tetra Octyl Ammonium Bromide
UHV	Ultra-High Vacuum
UV	Ultraviolet
XPS	X-ray Photoelectron Spectroscopy
XRD	X-ray Diffraction

Acknowledgement

First and foremost, I wish to thank my doctoral supervisor, Prof. Dr. Hermann A. Wegner for giving me the opportunity to carry out this work. This project grew from an urge to start up something completely new, into a far-fetched crazy idea, beclouded with lots of doubts, and finally into something very realistic and achievable. I also wish to appreciate the fact that he made himself available at all times, and always eager to discuss challenges, both chemistry-wise and on personal terms. This indeed, does not go unnoticed, as it provided me with an enabling environment to drive this challenging but interesting project to fruition. I also wish to extend my sincere gratitude to Prof. Dr. Bernd Smarsly for being the second examiner of this work.

Most importantly, I wish to thank my beloved mum, my ever caring siblings and my endearing girlfriend whose unwavering love could break the barriers of the distance between us, and who constantly reminded me who I am and kept me in track all through the duration of my doctorate program. Moreso, I sincerely wish to express my heartfelt gratitude to Gundula Talbot who has turned out to be family, and the brainbox behind my success. I hope you know that none of these would have been possible without your numerous sacrifices - and I am overtly grateful for this. Special thanks goes to Prof. Dr. Martin Muhler whose beliefs in me never faltered and gave me a solid scaffold to build a successful career in chemistry. I am also grateful to my friends, far and wide, whose words of encouragement went a long way to giving me the support I needed to successfully finish up my doctoral program.

In addition, I wish to thank the members of the Wegner group, more especially, Mari Janse Van Rensburg for introducing me to the group and strongly encouraging me to take up this bold step, which later turned out to be a good choice. And also to Daniel Kohrs, who gave me all the needed chemistry tips to carry out a very decent doctorate. My special thanks goes to the entire Nanocarbon subgroup alumni: Jan Griwatz, Jan Geldsetzer, Jannis Volkmann, and Felix Bernt, for the fruitful discussions during the subgroup meetings, which were helpful for the success of this work. Moreso, the current Nanocarbon subgroup: Rouven Fritzius, and Pia Mader for being such an accommodating colleagues and also contributing immensely to the chemistry. My overall thanks goes to the entire Wegner group: Dominic Schatz, Michel Grosse,

Konrad Averdunk, Kai Hanke, Christopher Leonhardt, and Silke Müsse for the nice and fruiful discussions in the coffee room.

Given the highly multidisciplinary nature of this doctoral thesis, my appreciation would be incomplete if not extended to the research groups of Prof. Dr. Smarsly, Prof. Dr. Janek, Prof. Dr. Schreiner, Prof. Dr. Spengler, and Prof. Dr. Göttlich whose collaborations and availability of analytical instruments made this project a huge success. Moreso, I wish to extend my gratitude to the secretaries: Anika Jägar, Michaela Richter and Maurice Monnard for assisting with administrative issues. Special thanks goes to Brigitte Weinl-Boulakhrouf, Dr. Heike Hausmann and all the members of the technical department who were always available even for spontaneous measurements. My gratitude also goes to all those unmentioned, but who contributed in one way or the other to the progress of this work. None of these would have been possible without you all, and for this, I say thank you!

Acknowledgement

Zuallererst möchte ich meinem Doktorvater, Prof. Dr. Hermann A. Wegner, dafür danken, dass er mir die Möglichkeit gegeben hat, diese Arbeit durchzuführen. Dieses Projekt entwickelte sich aus dem Drang, etwas völlig Neues zu beginnen, zu einer weit hergeholten verrückten Idee, die mit vielen Zweifeln behaftet war, und schließlich zu etwas sehr Realistischem und Erreichbarem. Ich möchte auch die Tatsache würdigen, dass er jederzeit zur Verfügung stand und immer bereit war, Herausforderungen zu besprechen, sowohl in Bezug auf die Chemie als auch auf persönliche Aspekte. Das ist in der Tat nicht unbemerkt geblieben, denn es hat mir ein günstiges Umfeld verschafft, um dieses anspruchsvolle, aber interessante Projekt zum Erfolg zu führen. Ich möchte auch Prof. Dr. Bernd Smarsly meinen aufrichtigen Dank dafür aussprechen, dass sie die zweite Prüferin dieser Arbeit war.

Vor allem möchte ich meiner geliebten Mutter, meinen stets fürsorglichen Geschwistern und meiner liebenswerten Freundin danken, deren unerschütterliche Liebe die Barrieren der Entfernung zwischen uns überwinden konnte und die mich ständig daran erinnerte, wer ich bin, und mich während der gesamten Dauer meines Promotionsprogramms auf Kurs hielt. Darüber hinaus möchte ich Gundula Talbot von Herzen danken, die sich als meine Familie erwiesen hat und die treibende Kraft hinter meinem Erfolg ist. Ich hoffe, Sie wissen, dass nichts von alledem ohne Ihre zahlreichen Opfer möglich gewesen wäre - und dafür bin ich Ihnen unendlich dankbar. Ein besonderer Dank geht an Prof. Dr. Martin Muhler, dessen Glaube an mich nie ins Wanken geriet und der mir ein solides Gerüst für eine erfolgreiche Karriere in der Chemie bot. Dankbar bin ich auch meinen Freunden aus nah und fern, die mir mit ihren aufmunternden Worten den nötigen Rückhalt gaben, um mein Promotionsstudium erfolgreich abzuschließen.

Außerdem möchte ich mich bei den Mitgliedern der Wegner-Gruppe bedanken, insbesondere bei Mari Janse Van Rensburg, die mich in die Gruppe eingeführt und mich nachdrücklich ermutigt hat, diesen mutigen Schritt zu wagen, der sich später als eine gute Entscheidung herausstellte. Und auch Daniel Kohrs, der mir alle nötigen Chemietipps gegeben hat, um eine sehr anständige Promotion zu machen. Mein besonderer Dank geht an die gesamten Alumni der Nanocarbon Subgroup: Jan Griwatz, Jan Geldsetzer, Jannis Volkmann und Felix Bernt, für die fruchtbaren

Diskussionen während der Untergruppentreffen, die für den Erfolg dieser Arbeit hilfreich waren. Mehr noch, die aktuelle Untergruppe Nanocarbon: Rouven Fritzius und Pia Mader für ihr Entgegenkommen und ihren enormen Beitrag zur Chemie. Mein allgemeiner Dank geht an die gesamte Wegner-Gruppe: Dominic Schatz, Michel Grosse, Konrad Averdunk, Kai Hanke, Christopher Leonhardt und Silke Müsse für die netten und fruchtbaren Gespräche in der Kaffeestube.

In Anbetracht des hochgradig multidisziplinären Charakters dieser Doktorarbeit wäre meine Anerkennung unvollständig, wenn ich nicht den Forschungsgruppen von Prof. Dr. Smarsly, Prof. Dr. Janek, Prof. Dr. Schreiner, Prof. Dr. Spengler und Prof. Dr. Göttlich danken würde, deren Zusammenarbeit und die Verfügbarkeit von Analyseinstrumenten dieses Projekt zu einem großen Erfolg machten. Darüber hinaus möchte ich mich bei den Sekretärinnen bedanken: Anika Jägar, Michaela Richter und Maurice Monnard für die Unterstützung bei administrativen Fragen. Mein besonderer Dank gilt Brigitte Weinl-Boulakhrouf, Dr. Heike Hausmann und allen Mitgliedern der technischen Abteilung, die auch für spontane Messungen immer zur Verfügung standen. Mein Dank gilt auch all jenen, die hier nicht genannt sind, aber in der einen oder anderen Weise zum Gelingen dieser Arbeit beigetragen haben. Ohne Sie alle wäre dies alles nicht möglich gewesen, und dafür sage ich Danke!

References

[1] N. Ukah, H. A. Wegner, *Chem. Eur.* **2024**.

[2] M.-C. Daniel, D. Astruc, *Chem. Rev.* **2004**, *104*, 293.

[3] D. M. P. Mingos (Ed.) *Structure and Bonding*, Springer International Publishing, Cham, **2014**.

[4] a) G. J. Leggett, *Nanoscale* **2012**, *4*, 1840; b) S. C. Singh, H. Zeng, *Sci. Adv. Mater.* **2012**, *4*, 368; c) H. Zeng, X.-W. Du, S. C. Singh, S. A. Kulinich, S. Yang, J. He, W. Cai, *Adv. Funct. Mater.* **2012**, *22*, 1333.

[5] a) N. G. Bastús, J. Comenge, V. Puntes, *Langmuir* **2011**, *27*, 11098; b) E. W. Edwards, M. Chanana, D. Wang, H. Möhwald, *Angew. Chem., Int. Ed.* **2008**, *120*, 326; c) J. Turkevich, P. C. Stevenson, J. Hillier, *Discuss. Faraday Soc.* **1951**, *11*, 55.

[6] S. Horikoshi, N. Serpone in *Microwaves in Catalysis* (Eds.: S. Horikoshi, N. Serpone), Wiley, **2015**, pp. 1–28.

[7] M. Chanana, L. M. Liz-Marzán, *Nanophotonics* **2012**, *1*, 199.

[8] S. Horikoshi, N. Serpone (Eds.) *Microwaves in Catalysis*, Wiley, **2015**.

[9] M. W. Brett, C. K. Gordon, J. Hardy, N. J. L. K. Davis, *ACS Phys. Chem. Au.* **2022**, *2*, 364.

[10] M. Tréguer-Delapierre, J. Majimel, S. Mornet, E. Duguet, S. Ravaine, *Gold Bull.* **2008**, *41*, 195.

[11] L. M. Liz-Marzán, *Langmuir* **2006**, *22*, 32.

[12] A. M. Funston, C. Novo, T. J. Davis, P. Mulvaney, *Nano Lett.* **2009**, *9*, 1651.

[13] J. Pérez-Juste, I. Pastoriza-Santos, L. M. Liz-Marzán, P. Mulvaney, *Coord. Chem. Rev.* **2005**, *249*, 1870.

[14] J. E. Millstone, S. J. Hurst, G. S. Métraux, J. I. Cutler, C. A. Mirkin, *Small* **2009**, *5*, 646.

[15] M. Tréguer-Delapierre, J. Majimel, S. Mornet, E. Duguet, S. Ravaine, *Gold Bull* **2008**, *41*, 195.

[16] K.-H. Su, Q.-H. Wei, X. Zhang, J. J. Mock, D. R. Smith, S. Schultz, *Nano Lett.* **2003**, *3*, 1087.

[17] V. Myroshnychenko, J. Rodríguez-Fernández, I. Pastoriza-Santos, A. M. Funston, C. Novo, P. Mulvaney, L. M. Liz-Marzán, F. J. García de Abajo, *Chem. Soc. Rev* **2008**, *37*, 1792.

[18] a) K. Kneipp, A. S. Haka, H. Kneipp, K. Badizadegan, N. Yoshizawa, C. Boone, K. E. Shafer-Peltier, J. T. Motz, R. R. Dasari, M. S. Feld, *Appl. Spectrosc.* **2002**, *56*, 150; b) J. T. Krug, G. D. Wang, S. R. Emory, S. Nie, *J. Am. Chem . Soc.* **1999**, *121*, 9208; c) C. E. Talley, J. B. Jackson, C. Oubre, N. K. Grady, C. W. Hollars, S. M. Lane, T. R. Huser, P. Nordlander, N. J. Halas, *Nano Lett.* **2005**, *5*, 1569.

[19] J. Jana, M. Ganguly, T. Pal, *RSC Adv.* **2016**, *6*, 86174.

[20] a) B. Sepúlveda, P. C. Angelomé, L. M. Lechuga, L. M. Liz-Marzán, *Nano Today* **2009**, *4*, 244; b) J. Liu, Y. Lu, *Angew. Chem., Int. Ed.* **2005**, *45*, 90; c) J.-S. Lee, M. S. Han, C. A. Mirkin, *Angew. Chem., Int. Ed.* **2007**, *46*, 4093.

[21] P. Mulvaney, *Langmuir* **1996**, *12*, 788.

[22] G. C. Papavassiliou, *J. Phys. Chem.* **1976**, *257O*, 241.

[23] C. Gao, X. Guo, L. Nie, X. Wu, L. Peng, J. Chen, *Int. J. Hydrogen Energy* **2023**, *48*, 2442.

[24] R. Jin, Y. Cao, C. A. Mirkin, K. L. Kelly, G. C. Schatz, J. G. Zheng, *Science* **2001**, *294*, 1901.

[25] *Phil. Trans. R. Soc.* **1857**, *147*, 145.

[26] S. D. Perrault, W. C. W. Chan, *J. Am. Chem . Soc.* **2009**, *131*, 17042.

[27] P. J. G. Goulet, R. B. Lennox, *J. Am. Chem . Soc.* **2010**, *132*, 9582.

[28] J. C. Love, L. A. Estroff, J. K. Kriebel, R. G. Nuzzo, G. M. Whitesides, *Chem. Rev.* **2005**, *105*, 1103.

[29] S. Engel, E.-C. Fritz, B. J. Ravoo, *Chem. Soc. Rev* **2017**, *46*, 2057.

[30] L. H. Dubois, R. G. Nuzzo, *Annu. Rev. Phys. Chem.* **1992**, *43*, 437.

[31] L. H. Dubois, B. R. Zegarski, R. G. Nuzzo, *J. Chem. Phys.* **1993**, *98*, 678.

[32] D. Fischer, A. Curioni, W. Andreoni, *Langmuir* **2003**, *19*, 3567.

[33] D. J. Lavrich, S. M. Wetterer, S. L. Bernasek, G. Scoles, *J. Phys. Chem. B* **1998**, *102*, 3456.

[34] G. Yang, N. A. Amro, Z. B. Starkewolfe, G.-Y. Liu, *Langmuir* **2004**, *20*, 3995.

[35] Y. Xia, G. M. Whitesides, *Angew. Chem., Int. Ed.* **1998**, *37*, 550.

[36] F. Schreiber, *Prog. Surf. Sci* **2000**, *65*, 151.

[37] H. Guan, C. Harris, S. Sun, *Acc. Chem. Res* **2023**, *56*, 1591.

[38] M. Wu, A. M. Vartanian, G. Chong, A. K. Pandiakumar, R. J. Hamers, R. Hernandez, C. J. Murphy, *J. Am. Chem . Soc.* **2019**, *141*, 4316.

[39] a) A. Badia, L. Cuccia, L. Demers, F. Morin, R. B. Lennox, *J. Am. Chem . Soc.* **1997**, *119*, 2682; b) M. J. Hostetler, J. J. Stokes, R. W. Murray, *Langmuir* **1996**, *12*, 3604; c) R. Paulini, B. L. Frankamp, V. M. Rotello, *Langmuir* **2002**, *18*, 2368; d) R. H. Terrill, T. A. Postlethwaite, C. Chen, C.-D. Poon, A. Terzis, A. Chen, J. E. Hutchison, M. R. Clark, G. Wignall, *J. Am. Chem . Soc.* **1995**, *117*, 12537; e) B. S. Zelakiewicz, G. C. Lica, M. L. Deacon, Y. Tong, *J. Am. Chem . Soc.* **2004**, *126*, 10053.

[40] A. S. Barnard, *Cryst. Growth Des.* **2013**, *13*, 5433.

[41] A. C. Templeton, M. J. Hostetler, E. K. Warmoth, S. Chen, C. M. Hartshorn, V. M. Krishnamurthy, M. D. E. Forbes, R. W. Murray, *J. Am. Chem . Soc.* **1998**, *120*, 4845.

[42] M. J. Hostetler, J. J. Stokes, R. W. Murray, *Langmuir* **1996**, *12*, 3604.

[43] a) W. D. Luedtke, U. Landman, *J. Phys. Chem. B* **1998**, *102*, 6566; b) W. D. Luedtke, U. Landman, *J. Phys. Chem.* **1996**, *100*, 13323; c) A. Badia, L. Cuccia, L. Demers, F. Morin, R. B. Lennox, *J. Am. Chem . Soc.* **1997**, *119*, 2682.

[44] S. Chen, K. Kimura, *Langmuir* **1999**, *15*, 1075.

[45] A. Henglein, M. Giersig, *J. Phys. Chem. B* **1999**, *103*, 9533.

[46] N. R. Jana, L. Gearheart, C. J. Murphy, *Langmuir* **2001**, *17*, 6782.

[47] S. Mann, *Angew. Chem., Int. Ed.* **2000**, *39*, 3392.

[48] a) M. Enayati, M.-W. Chang, F. Bragman, M. Edirisinghe, E. Stride, *Colloids Surfaces A.* **2011**, *382*, 154; b) X. Peng, L. Manna, W. Yang, J. Wickham, E. Scher, A. Kadavanich, A. P. Alivisatos, *Nature* **2000**, *404*, 59; c) Z. L. Wang, *J. Phys. Chem. B* **2000**, *104*, 1153.

[49] D. Reguera, R. K. Bowles, Y. Djikaev, H. Reiss, *J. Chem. Phys.* **2003**, *118*, 340.

[50] C. J. Murphy, N. R. Jana, *Adv. Mater.* **2002**, *14*, 80.

[51] M. N. Hopkinson, C. Richter, M. Schedler, F. Glorius, *Nature* **2014**, *510*, 485.

[52] A. J. Arduengo, R. Krafczyk, *Chemie in unserer Zeit* **1998**, *32*, 6.

[53] P. Bellotti, M. Koy, M. N. Hopkinson, F. Glorius, *Nat. Rev. Chem.* **2021**, *5*, 711.

[54] M. Koy, P. Bellotti, M. Das, F. Glorius, *Nat. Catal* **2021**, *4*, 352.

[55] G. Kaur, R. L. Thimes, J. P. Camden, D. M. Jenkins, *Chem. Comm.* **2022**, *58*, 13188.

[56] a) K. Salorinne, R. W. Y. Man, C.-H. Li, M. Taki, M. Nambo, C. M. Crudden, *Angew. Chem., Int. Ed.* **2017**, *56*, 6198; b) M. Ghosh, S. Khan, *ACS Catal.* **2023**, *13*, 9313.

[57] H. W. Wanzlick, *Angew. Chem., Int. Ed.* **1962**, *1*, 75.

[58] J. W. Runyon, O. Steinhof, H. V. R. Dias, J. C. Calabrese, W. J. Marshall, A. J. Arduengo, *Aust. J. Chem.* **2011**, *64*, 1165.

[59] C. Heinemann, T. Müller, Y. Apeloig, H. Schwarz, *J. Am. Chem . Soc.* **1996**, *118*, 2023.

[60] M. Ghosh, S. Khan, *ACS Catal.* **2023**, *13*, 9313.

[61] J. Vignolle, T. D. Tilley, *Chem. Comm.* **2009**, 7230.

[62] E. C. Hurst, K. Wilson, I. J. S. Fairlamb, V. Chechik, *New J. Chem.* **2009**, *33*, 1837.

[63] N. Zheng, J. Fan, G. D. Stucky, *J. Am. Chem. Soc.* **2006**, *128*, 6550.

[64] M. Rodríguez-Castillo, D. Laurencin, F. Tielens, A. van der Lee, S. Clément, Y. Guari, S. Richeter, *Dalton Trans.* **2014**, *43*, 5978.

[65] C. Richter, K. Schaepe, F. Glorius, B. J. Ravoo, *Chem. Comm.* **2014**, *50*, 3204.

[66] Z. Cao, D. Kim, D. Hong, Y. Yu, J. Xu, S. Lin, X. Wen, E. M. Nichols, K. Jeong, J. A. Reimer et al., *J. Am. Chem. Soc.* **2016**, *138*, 8120.

[67] X. Ling, S. Roland, M.-P. Pileni, *Chem. Mater.* **2015**, *27*, 414.

[68] X. Ling, N. Schaeffer, S. Roland, M.-P. Pileni, *Langmuir* **2013**, *29*, 12647.

[69] X. Ling, N. Schaeffer, S. Roland, M.-P. Pileni, *Langmuir* **2015**, *31*, 12873.

[70] S. Roland, X. Ling, M.-P. Pileni, *Langmuir* **2016**, *32*, 7683.

[71] J. Crespo, Y. Guari, A. Ibarra, J. Larionova, T. Lasanta, D. Laurencin, J. M. López-de-Luzuriaga, M. Monge, M. E. Olmos, S. Richeter, *Dalton Trans.* **2014**, *43*, 15713.

[72] S. G. Song, C. Satheeshkumar, J. Park, J. Ahn, T. Premkumar, Y. Lee, C. Song, *Macromolecules* **2014**, *47*, 6566.

[73] M. R. Narouz, C.-H. Li, A. Nazemi, C. M. Crudden, *Langmuir.* **2017**, *33*, 14211.

[74] R. W. Y. Man, C.-H. Li, M. W. A. MacLean, O. V. Zenkina, M. T. Zamora, L. N. Saunders, A. Rousina-Webb, M. Nambo, C. M. Crudden, *J. Am. Chem . Soc.* **2018**, *140*, 1576.

[75] R. Ye, A. V. Zhukhovitskiy, R. V. Kazantsev, S. C. Fakra, B. B. Wickemeyer, F. D. Toste, G. A. Somorjai, *J. Am. Chem. Soc.* **2018**, *140*, 4144.

[76] C. A. Smith, M. R. Narouz, P. A. Lummis, I. Singh, A. Nazemi, C.-H. Li, C. M. Crudden, *Chem. Rev.* **2019**, *119*, 4986.

[77] C. Boehme, G. Frenking, *Organometallics* **1998**, *17*, 5801.

[78] A. Inayeh, R. R. K. Groome, I. Singh, A. J. Veinot, F. C. de Lima, R. H. Miwa, C. M. Crudden, A. B. McLean, *Nat. Commun.* **2021**, *12*, 4034.

[79] a) N. A. Nosratabad, Z. Jin, L. Du, M. Thakur, H. Mattoussi, *Chem. Mater.* **2021**, *33*, 921; b) M. J. MacLeod, J. A. Johnson, *J. Am. Chem . Soc.* **2015**, *137*, 7974; c) S. R. Thomas, A. Casini, *J. Organomet. Chem* **2021**, *938*, 121743.

[80] G. Lovat, E. A. Doud, D. Lu, G. Kladnik, M. S. Inkpen, M. L. Steigerwald, D. Cvetko, M. S. Hybertsen, A. Morgante, X. Roy et al., *Chem. Sci.* **2019**, *10*, 930.

[81] C. R. Larrea, C. J. Baddeley, M. R. Narouz, N. J. Mosey, J. H. Horton, C. M. Crudden, *ChemPhysChem :* **2017**, *18*, 3536.

[82] A. Bakker, A. Timmer, E. Kolodzeiski, M. Freitag, H. Y. Gao, H. Mönig, S. Amirjalayer, F. Glorius, H. Fuchs, *J. Am. Chem . Soc.* **2018**, *140*, 11889.

[83] G. Wang, A. Rühling, S. Amirjalayer, M. Knor, J. B. Ernst, C. Richter, H.-J. Gao, A. Timmer, H.-Y. Gao, N. L. Doltsinis et al., *Nat. Chem.* **2017**, *9*, 152.

[84] a) F. Crasto de Lima, A. Fazzio, A. B. McLean, R. H. Miwa, *Phys. Chem. Chem. Phys.* **2020**, *22*, 21504; b) Q. Tang, D. Jiang, *Chem. Mater.* **2017**, *29*, 6908; c) M. Jain, U. Gerstmann, W. G. Schmidt, H. Aldahhak, *J. Comput. Chem.* **2022**, *43*, 413; d) L. Jiang, B. Zhang, G. Médard, A. P. Seitsonen, F. Haag, F. Allegretti, J. Reichert, B. Kuster, J. V. Barth, A. C. Papageorgiou, *Chem. Sci.* **2017**, *8*, 8301.

[85] R. L. Thimes, A. V. B. Santos, R. Chen, G. Kaur, L. Jensen, D. M. Jenkins, J. P. Camden, *J. Phys. Chem. Lett.* **2023**, *14*, 4219.

[86] J. Ren, M. Koy, H. Osthues, B. S. Lammers, C. Gutheil, M. Nyenhuis, Q. Zheng, Y. Xiao, L. Huang, A. Nalop et al., *Nat. Chem* **2023**, *15*, 1737.

[87] S. Clair, D. G. de Oteyza, *Chem. Rev.* **2019**, *119*, 4717.

[88] M. Di Giovannantonio, M. El Garah, J. Lipton-Duffin, V. Meunier, L. Cardenas, Y. Fagot Revurat, A. Cossaro, A. Verdini, D. F. Perepichka, F. Rosei et al., *ACS nano* **2013**, *7*, 8190.

[89] M. Di Giovannantonio, M. Tomellini, J. Lipton-Duffin, G. Galeotti, M. Ebrahimi, A. Cossaro, A. Verdini, N. Kharche, V. Meunier, G. Vasseur et al., *J. Am. Chem . Soc.* **2016**, *138*, 16696.

[90] a) J. Eichhorn, D. Nieckarz, O. Ochs, D. Samanta, M. Schmittel, P. J. Szabelski, M. Lackinger, *ACS nano* **2014**, *8*, 7880; b) M. Fritton, D. A. Duncan, P. S. Deimel, A. Rastgoo-Lahrood, F. Allegretti, J. V. Barth, W. M. Heckl, J. Björk, M. Lackinger, *J. Am. Chem . Soc.* **2019**, *141*, 4824; c) Z. Huang, M. L. Tang, *J. Am. Chem . Soc.* **2017**, *139*, 9412.

[91] L. Grill, S. Hecht, *Nat. Chem* **2020**, *12*, 115.

[92] L. Grossmann, D. A. Duncan, S. P. Jarvis, R. G. Jones, S. De, J. Rosen, M. Schmittel, W. M. Heckl, J. Björk, M. Lackinger, *Nanoscale Horiz* **2021**, *7*, 51.

[93] Z. Huang, Z. Xu, T. Huang, V. Gray, K. Moth-Poulsen, T. Lian, M. L. Tang, *J. Am. Chem . Soc.* **2020**, *142*, 17581.

[94] C. J. Judd, F. L. Q. Junqueira, S. L. Haddow, N. R. Champness, D. A. Duncan, R. G. Jones, A. Saywell, *Commun. Chem* **2020**, *3*, 166.

[95] P. Ruffieux, S. Wang, B. Yang, C. Sánchez-Sánchez, J. Liu, T. Dienel, L. Talirz, P. Shinde, C. A. Pignedoli, D. Passerone et al., *Nature* **2016**, *531*, 489.

[96] Q. Shen, H.-Y. Gao, H. Fuchs, *Nano Today* **2017**, *13*, 77.

[97] K. A. Simonov, N. A. Vinogradov, A. S. Vinogradov, A. V. Generalov, E. M. Zagrebina, G. I. Svirskiy, A. A. Cafolla, T. Carpy, J. P. Cunniffe, T. Taketsugu et al., *ACS nano* **2015**, *9*, 8997.

[98] M. M. Blake, S. U. Nanayakkara, S. A. Claridge, L. C. Fernández-Torres, E. C. H. Sykes, P. S. Weiss, *J. Phys. Chem. A* **2009**, *113*, 13167.

[99] Q. Zhong, J. Jung, D. Kohrs, L. A. Kaczmarek, D. Ebeling, D. Mollenhauer, H. A. Wegner, A. Schirmeisen, *J. Am. Chem. Soc.* **2024**, *146*, 1849.

[100] Q. Shen, H.-Y. Gao, H. Fuchs, *Nano Today* **2017**, *13*, 77.

[101] Q. Zhong, A. Ihle, S. Ahles, H. A. Wegner, A. Schirmeisen, D. Ebeling, *Nat. Chem* **2021**, *13*, 1133.

[102] M. Matena, T. Riehm, M. Stöhr, T. A. Jung, L. H. Gade, *Angew. Chem., Int. Ed.* **2008**, *47*, 2414.

[103] a) J. F. Dienstmaier, D. D. Medina, M. Dogru, P. Knochel, T. Bein, W. M. Heckl, M. Lackinger, *ACS nano* **2012**, *6*, 7234; b) O. Ourdjini, R. Pawlak, M. Abel, S. Clair, L. Chen, N. Bergeon, M. Sassi, V. Oison, J.-M. Debierre, R. Coratger et al., *Phys. Rev. B* **2011**, *84*; c) N. A. A. Zwaneveld, R. Pawlak, M. Abel, D. Catalin, D. Gigmes, D. Bertin, L. Porte, *J. Am. Chem. Soc.* **2008**, *130*, 6678.

[104] S. Weigelt, C. Bombis, C. Busse, M. M. Knudsen, K. V. Gothelf, E. Laegsgaard, F. Besenbacher, T. R. Linderoth, *ACS nano* **2008**, *2*, 651.

[105] a) M. Treier, N. V. Richardson, R. Fasel, *J. Am. Chem . Soc.* **2008**, *130*, 14054; b) A. C. Marele, R. Mas-Ballesté, L. Terracciano, J. Rodríguez-Fernández, I. Berlanga, S. S. Alexandre, R. Otero, J. M. Gallego, F. Zamora, J. M. Gómez-Rodríguez, *Chem. Comm.* **2012**, *48*, 6779.

[106] Q. Sun, C. Zhang, Z. Li, H. Kong, Q. Tan, A. Hu, W. Xu, *J. Am. Chem. Soc.* **2013**, *135*, 8448.

[107] a) M. Treier, C. A. Pignedoli, T. Laino, R. Rieger, K. Müllen, D. Passerone, R. Fasel, *Nat. Chem* **2011**, *3*, 61; b) G. Otero, G. Biddau, C. Sánchez-Sánchez, R. Caillard, M. F. López, C. Rogero, F. J. Palomares, N. Cabello, M. A. Basanta, J. Ortega et al., *Nature* **2008**, *454*, 865.

[108] F. Bebensee, C. Bombis, S.-R. Vadapoo, J. R. Cramer, F. Besenbacher, K. V. Gothelf, T. R. Linderoth, *J. Am. Chem. Soc.* **2013**, *135*, 2136.

[109] O. Díaz Arado, H. Mönig, H. Wagner, J.-H. Franke, G. Langewisch, P. A. Held, A. Studer, H. Fuchs, *ACS nano* **2013**, *7*, 8509.

[110] a) C. Sambiagio, S. P. Marsden, A. J. Blacker, P. C. McGowan, *Chem. Soc. Rev* **2014**, *43*, 3525; b) E. Sperotto, G. P. M. van Klink, G. van Koten, J. G. de Vries, *Dalton Trans.* **2010**, *39*, 10338.

[111] J. A. Lipton-Duffin, O. Ivasenko, D. F. Perepichka, F. Rosei, *Small* **2009**, *5*, 592.

[112] a) M. Bieri, M.-T. Nguyen, O. Gröning, J. Cai, M. Treier, K. Aït-Mansour, P. Ruffieux, C. A. Pignedoli, D. Passerone, M. Kastler et al., *J. Am. Chem. Soc.* **2010**, *132*, 16669; b) G. S. McCarty, P. S. Weiss, *J. Am. Chem . Soc.* **2004**, *126*, 16772; c) M.-T. Nguyen, C. A. Pignedoli, D. Passerone, *Phys. Chem. Chem. Phys.* **2011**, *13*, 154.

[113] M. Xi, B. E. Bent, *Surf. Sci.* **1992**, *278*, 19.

[114] E. A. Lewis, C. J. Murphy, M. L. Liriano, E. C. H. Sykes, *Chem. Comm.* **2014**, *50*, 1006.

[115] H. Walch, R. Gutzler, T. Sirtl, G. Eder, M. Lackinger, *J. Phys. Chem. C* **2010**, *114*, 12604.

[116] J. Park, K. Y. Kim, K.-H. Chung, J. K. Yoon, H. Kim, S. Han, S.-J. Kahng, *J. Phys. Chem. C* **2011**, *115*, 14834.

[117] W. Wang, X. Shi, S. Wang, M. A. van Hove, N. Lin, *J. Am. Chem . Soc.* **2011**, *133*, 13264.

[118] M. Chen, J. Xiao, H.-P. Steinrück, S. Wang, W. Wang, N. Lin, W. Hieringer, J. M. Gottfried, *J. Phys. Chem. C* **2014**, *118*, 6820.

[119] L. Dong, P. N. Liu, N. Lin, *Acc. Chem. Res* **2015**, *48*, 2765.